# Solar geoengineering can alleviate climate change pressures on crop yields

# Solar geoengineering can alleviate climate change pressures on crop yields

Yuanchao Fan[1,2,*], Jerry Tjiputra[1], Helene Muri[3], Danica Lombardozzi[4], ChangEui Park[5], Shengjun Wu[6], David Keith[7,8]

[1]NORCE Norwegian Research Centre and Bjerknes Centre for Climate Research, Bergen, Norway, [2]Center for the Environment, Faculty of Arts & Sciences, Harvard University, Cambridge, MA, USA, [3]Industrial Ecology Programme, Department of Energy and Process Engineering, Norwegian University of Science and Technology, Trondheim, Norway, [4]Climate and Global Dynamics Laboratory, National Center for Atmospheric Research, Boulder, CO, USA, [5]Department of Environmental Planning, Graduate School of Environmental Studies, Seoul National University, Seoul, Republic of Korea, [6]Three Gorges Research Center for Ecology and Environment, Chongqing Institute of Green and Intelligent Technology, Chinese Academy of Sciences, Chongqing, China, [7]John A. Paulson School of Engineering and Applied Sciences, Harvard University, Cambridge, MA, USA, [8]John F. Kennedy School of Government, Harvard University, Cambridge, MA, USA.

*Corresponding author: ycfan@seas.harvard.edu

## Abstract

Solar geoengineering (SG) and $CO_2$ emissions reduction (ER) can each alleviate anthropogenic climate change, but their impacts on food security have not yet been fully understood. Using an advanced crop model within an Earth system model, we analysed yield responses of six major crops to three SG technologies and ER when they provide roughly the same reduction in radiative forcing and assume the same land use. We found sharply distinct yield responses to changes in radiation, moisture and $CO_2$, but comparable, significant cooling benefits for crop yields by all four methods. Overall, global yields increase ~10% under the three SGs and decrease 5% under ER, the latter primarily due to reduced $CO_2$ fertilization, relative to business-as-usual by late 21$^{st}$ century. Relative humidity dominates the hydrological effect on yields of rainfed crops, with little contribution from precipitation. The net insolation effect is negligible across all SGs, contrary to previous findings.

Climate intervention through solar geoengineering (SG) has been proposed as a complementary strategy for mitigating anthropogenic greenhouse gas induced warming, particularly when discussing the ambitious climate target set in the Paris Agreement[1,2]. SG and related techniques typically use aerosols to counterbalance some of the radiative forcing from long-lived greenhouse gases, either by reflecting more shortwave solar radiation away from Earth, such as Stratospheric Aerosol Injection (SAI)[3] and Marine Sky Brightening (MSB, see nomenclature in Methods)[4,5], or by enhancing Earth's longwave radiation towards space through Cirrus Cloud Thinning (CCT)[5] (strictly CCT is not "solar" but hereafter we will refer to all SG-related methods as SG). Although the number of modelling studies on the method and impact of SGs has increased rapidly since Crutzen's 2006 paper[3], and the launch of the Geoengineering Model Intercomparison Project (GeoMIP)[6] in particular, the majority of them focused on the physical responses of the atmosphere, ocean and cryosphere components of the climate system to these large-scale interventions[7,8]. The impact of SG on terrestrial ecosystems and agriculture remains poorly understood[9]. To date, only a few modelling studies have investigated the regional[10–13] or global[14,15] impact of a specific SG such as SAI on the yield of certain crops. Inconsistent findings on the mechanisms and effectiveness of SAI, e.g., the roles of temperature and radiation, on global crop yield have emerged in the literature[14,15] (though these studies applied notably different approaches). A global assessment of agricultural responses to multiple SG methods, and a direct comparison of the agricultural impacts of SGs and $CO_2$ emissions reduction (hereafter ER) under similar radiative forcing pathways, were both needed.

We took a stepwise approach (Fig. 1a) to understand crop yield responses to our selected scenarios. We first implemented three SGs (SAI, MSB, CCT) on top of the representative concentration pathway 8.5 (RCP85) to achieve the same net reduction in radiative forcing as RCP45, which is then referred to as our ER scenario, using the NorESM1-ME[16] climate model. Each of the three SG methods does have multiple design choices[17] that could result in different climate responses, but here we used one instance of idealized experiment for SAI, MSB and CCT, respectively, and focused on cross-SG-method comparison in our sensitivity analysis. We then applied the climate scenarios to the CLM5[18] process-based global gridded crop model to determine the impact of SGs and ER on the yield of six major crops (maize, sugarcane, wheat, rice, soy and cotton) that produce food, bioenergy and fibre. For crop yield modelling, we note potential uncertainties with respect to changing land use pathways under

different emission scenarios[19]. According to a scenario matrix framework and the standard configuration in ScenarioMIP[20], we combined the RCP85 climate with the Shared Socioeconomic Pathway 5 (SSP5) land use as the default configuration for RCP85. All SGs (SAI, MSB, CCT) and ER ($RCP45_{(SSP5LU)}$) scenarios were simulated with the same SSP5 land use as in RCP85 to exclude the effect of land-use change for comparison between SGs and ER. We performed additional simulations that apply combinations of climate, $CO_2$ and land use (Table 1), to isolate the physiological effect of $CO_2$ and decompose climate-only effects (Fig. 1a), and to assess potential uncertainties associated with changing land use for ER (e.g., from SSP5 to SSP2, see Supplementary Information sections I and II).

Our results show that without mitigation, annual average warming over land and growing season warming over cropping areas reach 5.4°C and 6 °C, respectively, above the preindustrial levels by the end of 21st century (2075-2099 mean; Fig. 1b), within the range of projections of the Intergovernmental Panel on Climate Change Fifth Assessment Report (IPCC AR5)[21]. Simulations show substantial changes in crop yields in response to changes in climate, $CO_2$ concentration, land use and crop management trends under the different scenarios (Fig. 1f for global trends, Supplementary Fig. 1 for crop-specific trends). We validated CLM5 modelled crop yields during 2006-2018 with the FAOSTAT data[22], which showed reasonable fidelity in simulated levels of global total production and average yields (Fig. 2). More detailed global and regional evaluation of CLM5 crop simulations can be found in Lombardozzi et al.[18].

We quantified the relative effects of surface air temperature, direct and diffuse solar radiation, precipitation, and relative humidity on each crop type under each of the SG and ER scenarios compared to reference case RCP85, by conducting multiple linear regression (MLR) for each grid cell and each crop type on 2020-2099 time series data. We found the mean partial and total climate effects for the globe, and then used a Monte Carlo or Bootstrap approach[23] to resample and derive a confidence interval for each MLR coefficient (Fig. 1a, details in Methods). To estimate the net impact of ER, the climate-only effects were merged with the effect of reduced $CO_2$ from RCP85 to RCP45. Finally, we compared SGs and ER to assess the mechanisms and effectiveness of the different scenarios for agricultural production in the 21st century.

## Partial and total climate effects

The different cooling strategies result in spatially and temporally heterogeneous impacts on crop yield in the 21st century (Figs. 3-5). Reduced air temperature has consistently strong positive effect on global average yield under all scenarios (Fig. 3). In contrast to the similar temperature effects, the different scenarios offer distinct radiation and moisture-related effects and trends across regions and time. The moisture effect, dominated by changes in relative humidity rather than precipitation, drives much of the interannual variability in the total climate effect. Remarkably, in ER it reaches a comparable level to the temperature effect after year 2050 (Fig. 3d). The net effect of relative humidity is closely linked to vapour pressure deficit, which is important for crop growth and yield[24,25]. There are simultaneous drops in precipitation and relative humidity around the year 2067 under RCP85 indicating a dry period (Fig. 1d). The SGs and ER scenarios all have increased relative humidity compared to RCP85 around 2067. Increased relative humidity reduces vapour pressure deficit and alleviates water stress, which explains the synchronous peak of relative humidity effect under all scenarios during this dry period (Fig. 3a-d). The net effect of altered radiation regimes on crop yield is relatively small in all scenarios, due to the opposing changes in direct and diffuse radiation components. Under SAI, the positive effect of increased diffuse radiation on yields largely compensates for the loss caused by reduced direct sunlight, and in some cases contributes to increased yields (Fig. 3a,e). In CCT, contrastingly, the slight increase in direct radiation versus decrease in diffuse radiation from the reduced layer of thin ice clouds in the upper troposphere brings marginal net increase in global yield (Fig. 3c,e). MSB shows weaker radiation effects than SAI (Fig. 3b,e), considering the aerosol forcing is only applied over the oceans.

Crop-specific analysis shows diverse responses of the six crops to changes in different climate variables. The yield increments of most crops are primarily driven by cooling (Fig. 4). The exceptions are wheat and rice, which are particularly insensitive to temperature (Supplementary Fig. 1) yet respond strongly to changes in radiation and relative humidity under ER, SAI, and MSB when not irrigated (Fig. 4a). Separating irrigated and rainfed crops shows that the effects of temperature and radiation are dependent on water stress level. Eliminating water stress through irrigation dampens the effects of temperature and radiation for most crops, and for some crops reduces the

total effect by more than 50% (Fig. 4a,b). Most rainfed crops show significant responses to increased relative humidity, with larger increases under ER than SGs (Fig. 3, Fig. 4a). CCT shows a muted crop relative humidity response (Fig. 3e, Fig. 4a) because it causes only small changes in global average humidity compared to RCP85 after 2075 (Fig. 1d). Precipitation exerts minimal effects on most rainfed crops after accounting for temperature, radiation, and relative humidity effects, which holds even if removing relative humidity from the regression (Eq. 1 in Methods). The minor role of precipitation reflects the complexity of crop water availability and use due to variable runoff, drainage and evaporation[26]. As relative humidity regulates evaporation and plant water use through stomatal control, increased relative humidity alleviates water stress for rainfed crops at a given temperature; lower relative humidity indicates higher vapour pressure deficit which may trigger stomatal closure[25,27,28] and reduces crop growth and yield[26]. Our finding of the dominant role of relative humidity rather than precipitation on crop productivity is consistent with a previous SAI study that considered both variables[11] (other SAI studies neglected relative humidity[10,14,15]) and with other studies on the role of relative humidity or vapour pressure deficit on vegetation and crop productivity[24,25,27].

Overall, the methods that promote cooling and at the same time alleviate water stress, which occurs in Central America and South America in most scenarios (Supplementary Fig. 2), will likely result in the highest yield gains, particularly for maize, soy, and sugarcane in the Global South (Fig. 5, Extended Data Figs. 1-2). Globally, higher relative humidity increases yields by ~3% under the SGs, and 8% under ER (2075-2099 mean). By comparing the different SGs and ER, our results suggest that evaluating climate impacts on water availability and agricultural productivity should not focus only on precipitation, but rather on the balance of water input and water loss. Taking relative humidity into account forces a revaluation of previous assessments that SAI would have a negative impact on crop yield due to reduced precipitation[7,10]; indeed we found little impact of precipitation reduction in India and China, and even yield increase in South America.

## Reduced $CO_2$ fertilization under ER

The combined cooler temperatures and higher humidity under ER (Fig. 1) would lead to increased global yield compared to the SG scenarios if one neglects the impact of $CO_2$ fertilization (i.e., $RCP45_{(SSP5LU)} - RCP85_{(45CO2)}$). However, the reduced crop yields because of lower $CO_2$ concentrations under ER outweigh the temperature and humidity benefits regionally (Extended Data Fig. 1d) and globally (Fig. 3, Fig. 4) for most $C_3$ crops, resulting in a global marginal loss of yield by -5% during 2075-2099 ($RCP45_{(SSP5LU)} - RCP85$; Fig. 3e, Supplementary Table 1). Our regression analysis shows doubling $CO_2$ concentration from 380 to 760 ppm while other climate variables remain the same as RCP85 increases global yield by 9%, 16%, 20%, 25% and 31% for maize, sugarcane, rice, cotton and wheat, respectively, and up to 75% for soy (see Methods and Extended Data Fig. 3). These $CO_2$ fertilization factors, except for soy, are very similar to those used in the DSSAT model and related SG studies[10,14] and those observed in the Free-air $CO_2$ enrichment experiments (per 200 ppm $CO_2$ increment)[29,30]. Although elevated $CO_2$ can stimulate soy's photosynthetic capacity by 60-80% as it is not limited by nitrogen, several plant-level physiological feedbacks limit soy's investment for reproduction and thus reduce the yield sensitivity[31], but this mechanism is not included in CLM5. Halving the yield response of soy to $CO_2$ would make it closer to observations and other crops (Extended Data Fig. 3) but does not change our conclusion on the comparative effects of ER and SG. The higher sensitivity of $C_3$ crops (soy, wheat, rice and cotton) to $CO_2$ concentrations than $C_4$ crops (maize and sugarcane) is consistent with observations[32], although significant spatial heterogeneity exists even for a given crop type (Extended Data Figs. 1-2), which is likely related to changing soil nutrient and moisture conditions[33]. Comparison of irrigated and rainfed crops reveals that eliminating water stress by irrigation reduces the $CO_2$ effect for most crops (Fig. 4); this is related to the role of elevated $CO_2$ in improving plant water-use efficiency (and vice versa) and consistent with observations where the effect of $CO_2$ on crops decreases with higher water availability[30].

Our quantitative analysis shows the reduced $CO_2$ fertilization under ER undermines its cooling and humidity benefits, making SGs robustly more effective at increasing global yield (11%, 9% and 11% for SAI, MSB and CCT, respectively, during 2075-2099; Fig. 3e, Supplementary Table 1), though they have distinct mechanisms.

## Limitations and uncertainties

Our results are only as good as our assumptions. The use of any SG technology would entail many design choices that would shape the spatial and temporal distribution of radiative forcing along with many of its side effects[17]. The spatial distribution of sensitivity to MSB and CCT interventions, in particular, depends on aerosol-cloud interactions that are poorly constrained by observations[34]. The meridional distribution of SAI is a design choice with important consequences for hydrology[35].

NorESM1-ME showed satisfactory performance on climate projections in CMIP5[36] and GeoMIP5[37] and CLM5 has also been rigorously evaluated[18,38,39]. Nevertheless, absolute prediction of future crop yield is hindered by uncertainties in estimating future climates or in the forcing dataset[40], in the crop model parameterizations[18], and in assumptions regarding country-specific differences in agricultural practice and adaptation[41]. The CLM5 crop model needs improvements in allocation and temperature-triggered phenology, as well as biological nitrogen fixation for soy[18], and can be further improved towards better representation of crop response to extreme weather events[42] and to $CO_2$ fertilization. Lombardozzi et al.[18] showed the CLM5 simulated crop yield response to $CO_2$ enrichment was nearly double observations from FACE experiments[29] and that irrigated crops had higher response than rainfed crops was the opposite of observations. But our independent evaluation of CLM5 against observations shows reasonable $CO_2$ effect for most crops (except for soy, see above section) whether irrigated or not. There are several reasons for this difference, including different forcing data and different climate contexts of evaluation: Lombardozzi et al.[18] used the GSWP3 forcing for a historical scenario (added 200 ppm $CO_2$ from 1990 to 2010 while other climate variables remained the same), whereas our simulations used coupled model forcing for future scenarios. Moreover, we found abnormal sub-daily covariance of surface air temperature and relative humidity in the GSWP3 dataset resulting in significantly higher moist heat stress (measured by wet-bulb temperature[43]) for tropical, subtropical and some midlatitude regions than several other reanalysis datasets (not shown). The abnormal forcing data used in Lombardozzi et al.[18] could affect the energy and water cycle in CLM5[40] and contribute to the differences in simulated yield responses to $CO_2$ compared to our crop simulations which are more consistent with observations. In CMIP5[36] coupled simulations, the CLM model showed weaker

land carbon response to $CO_2$ than other land surface schemes, and CLM5 has an improved response to $CO_2$ compared to older versions of CLM[44].

Could our model undercount the effect of dimming for SAI? One must consider the radiative properties of aerosols when assessing the impact of SAI. The same increase in stratospheric aerosol optical depth (SAOD) could produce different amounts of down-scattering depending on aerosol size distribution. All else equal, a higher diffuse radiation fraction enhances canopy absorption of photosynthetic active radiation[45] and carbon uptake in forests and croplands[46], and also promotes crop yield due to enhanced radiation use efficiency[47]. Thus, per unit increase in SAOD, the SAI with relatively more down-scattering aerosols and higher proportional increase in diffuse radiation should have larger yields. Proctor et al.[15] examined observations of SAOD and crop yield finding a strong net negative insolation effect offsetting the positive cooling effect of SAI on crop yield. Their study rested on two important assumptions: (i) homogeneous linear insolation effect of SAOD taken from the Pinatubo eruption (which had less down-scattering than other volcanic eruptions like the El Chichón[15], and less than our model SAI experiment); (ii) their reference scenario was RCP45 instead of RCP85, and thus their cooling effect of SAI was relatively weaker than our case. Our sensitivity analysis of modeled crop responses to radiative changes (Extended Data Fig. 4) show that the negative effect of reduced direct radiation could overtake the positive diffuse radiation effect if the direct and diffuse components decrease (e.g., -20%) and increase (e.g., +20%) proportionally. When applying our MLR coefficients to volcanic-induced changes in direct and diffuse radiation after the Pinatubo eruption (-21% direct and +20% diffuse, from Proctor et al.[15]), we found similar net negative insolation effects on maize (-8.9%), rice (-6.7%), soy (-3.6%) and wheat (-2.7%) to those shown in Proctor et al.[15] (see their Fig. 3). In our SAI experiment, the non-proportional opposing changes in direct (-11 W $m^{-2}$ or -12%) and diffuse (+7 W $m^{-2}$ or +20%, 2075-2099 mean) radiation relative to RCP85 (Fig. 1c) indicate more down-scattering, resulting in negligible net insolation effects on most crops (Fig. 4), although small regional variations exist (Extended Data Figs. 1-2). We also found the effects of opposing changes in direct and diffuse radiation largely would cancel out each other in MSB and CCT scenarios. Therefore, the difference between our results and those of Proctor et al.[15] is not due to differences in crop sensitivity to the radiative changes in CLM5 versus observations, but mainly due to different radiative changes in our SG experiments from those after the

198 Pinatubo eruption. Our study highlights the importance of optimizing aerosol particle size distribution. Given that
199 the increase in diffuse light from SAI is somewhat adjustable through design choices[48], the impacts of a particular
200 volcanic eruption is a limited analog for SAI deployment.

201 Besides crop's physiological responses to climate and $CO_2$, agricultural management such as irrigation and
202 nitrogen fertilization are known to significantly impact crop productivity[49], but have not been fully considered in
203 previous solar geoengineering studies. Our goal was to isolate the effect of ER (climate and $CO_2$ only) on crop
204 yield. But ER will likely be linked to changes in land use, although future land use and agricultural practice are
205 hard to predict under any mitigation scenario. We examined the potential importance of land use change (LUC)
206 by adopting the IPCC standard, in which RCP85 is associated with SSP5 and RCP45 with SSP2[20]. Under these
207 conditions, the relative advantage of SGs over ER in terms of effect on global average yield (Supplementary Fig.
208 3a) and on global total production (Supplementary Table 1) become smaller but still robust. This is mainly due to
209 higher nitrogen fertilizer use in SSP2 than SSP5 (Fig. 1e) to balance the demands for food, feed and bioenergy
210 production with limited land area available for agriculture[50], which largely compensates for the weaker $CO_2$
211 fertilization effect in ER for most crops (Supplementary Fig. 3b-c). In our LUC analysis, yields of most crops,
212 except soy and cotton, are sensitive to increased nitrogen fertilizer usage (Supplementary Fig. 4). Other
213 confounding factors on crop responses to LUC include the effective climate shift caused by changing crop spatial
214 distribution from SSP5 to SSP2 (Supplementary Fig. 5-6) and changing irrigated fraction of each crop type (Fig.
215 1e and Supplementary Fig. 7-8). The LUC analysis implies that the advantage of SGs over ER depends on the
216 assumption that their use is not associated with other management or technological changes that might increase or
217 reduce crop yields.

218 **Conclusions**

219 Cooling is the primary driver of increases in crop yields under both SG and ER relative to RCP85. An important
220 secondary driver is the interannual variability in relative humidity under different scenarios. The strong cooling
221 and humidity benefits under ER is counteracted by its reduced $CO_2$ fertilization, leading to reduced yields

compared to the SGs. The net impact of changes in direct and diffuse radiation is small under all scenarios. Overall yields in the Global South benefit consistently from all scenarios, particularly for maize, soy and sugarcane, whereas wheat and rice are less sensitive to the cooling induced by SGs or ER in general.

Our conclusions depend on other unaddressed uncertainties in the models. Future efforts could extend this assessment by using different climate and crop models and forcing datasets. Climate mitigation ultimately depends on synergistic efforts from all social-economic sectors, considering the advantages of multiple solutions and their potential risks. Policymakers should seek a balanced approach to sustaining global production of food, bioenergy and fibre, considering the various effects of different mechanisms offered by SGs and ER in regulating the carbon, water and nutrient cycles in agricultural systems.

## Methods

Among the GeoMIP5 models, the three SGs (SAI, MSB, CCT) were simulated consistently only in the Norwegian Earth System Model version 1 (NorESM1-ME), providing a unique experiment set for comparing multiple SG methods in this study. Even the current GeoMIP6 does not have consistently designed experiments for SAI, MSB and CCT like those done by NorESM1-ME. The general climate features in three SGs, together with RCP45 and RCP85, have been thoroughly analysed in prior studies[5,8,51]. Details on SG implementations are found in Muri et al.[5]. In the MSB experiment, sea salt emissions were increased in both clear-sky and cloudy regions to actively draw upon the direct effect of sea salt aerosols in addition to the indirect effect through marine cloud processes, which is thus referred to as marine sky brightening instead of more commonly studied marine cloud brightening[1,4]. We note that each SG method itself has multiple design choices that could result in different climate and crop yield responses. Such intra-method variations for a specific SG technique is beyond the scope of this study and we focused on cross-SG-method comparison for our yield impact analysis. Here we rerun these simulations with output of high-frequency (hourly to 3-hourly) coupler history data in order to force the crop model. We chose Community Land Model version 5 (CLM5) as the crop model because CLM4 (within NorESM1-ME) does not have prognostic crop types required for this study. CLM5 is a global land model that represents changing distributions of multiple crop types and management through time[18]. This enabled us to simulate transient yields of the six common crops under different climate and land use scenarios.

### Model experiments

We used the fully coupled emission driven NorESM1-ME climate model to simulate the three SG scenarios (SAI, MSB, CCT) from 2020-2099, as well as two reference climate scenarios RCP45 and RCP85 from 2006-2099 at 1.9° latitude × 2.5° longitude resolution. The SAI, MSB and CCT schemes were implemented on top of a RCP85 baseline in a consistent manner, such that the change in radiative forcing in RCP85 was reduced to that comparable to the RCP45 scenario (ER) during the period 2020-2099. The NorESM1-ME coupler history data of these five climate scenarios were downscaled to 0.9° latitude × 1.25° longitude resolution and then used as

meteorological forcing to drive CLM5 with prognostic crops (CLM5-crop). The CLM5-crop represents the growth, yield and agricultural management of six major crops: maize, wheat, rice, soy, sugarcane and cotton. Each crop is split to irrigated and rainfed subtypes, varying by region. Soy and maize additionally have temperate and tropical cultivars, which were merged in the post-processing before the analysis. The Land-Use Harmonization (LUH2) transient land cover data[52] provided yearly surface boundary conditions of SSP2 and SSP5 scenarios at 0.9° latitude × 1.25° longitude resolution. All SGs and ER used the SSP5 land use as in RCP85 to facilitate inter-scenario comparison for quantifying the effects of changes in different climate variables on crop yield. We additionally set up two offline simulations: one combines RCP85 climate and RCP45 atmospheric $CO_2$ concentrations to isolate $CO_2$ effects, and another combines RCP45 climate and SSP2 land use to represent a scenario in which ER is associated with changing land use and related effects (compared to RCP85). Altogether, we conducted seven experiments as summarized in Table 1. We modified the history module of CLM5 to output crop-specific yield data with a four-dimensional variable "CROPPROD1C_HARV_CFT" that contains per grid cell harvest flux over time to 1-year crop product pool for each of the six crop types and for rainfed and irrigated subtypes separately.

**Crop model evaluation**

CLM5 simulated crop production and per hectare yield were compared with FAOSTAT data[22] (Food and Agriculture Organization of the United Nations corporate Statistical Database) from 2006 to 2018 (Fig. 2). The FAO crop production quantities were first converted to dry matter using crop-specific dry-to-fresh weight ratios[53]. Sugarcane yield was expressed as sucrose amount after dividing FAO cane yield by a tonnes cane per tonne sugar ratio of 8. Cotton yield represents cotton lint production divided by its harvested area. CLM5 modelled crop harvest amounts (in g C $m^{-2}$) under RCP85 from 2006-2018 were converted to dry matter using a carbon to dry weight ratio of 0.45 and harvest efficiency of 85% according to CLM5 tech note (https://escomp.github.io/ctsm-docs/doc/build/html/tech_note/). Overall, the accumulative production (million tonnes $year^{-1}$) simulated for most crops is within ±20% difference from FAO data, with an exception of rice, whose overestimation exceeds 30%. Biases exist in crop cultivation area of SSP5 land use time series data for years 2006-2018 compared with the

harvested area of FAOSTAT, especially for wheat and cotton, although their simulated productions are close to observation (Fig. 2a). Overall, the simulated yield per hectare aligns reasonably well with FAO data (Fig. 2b). For soy and rice, the overestimation is less than 20% in the validation period, and for maize, wheat and sugarcane the underestimations are less than 12%. Larger overestimation for cotton yield (80%) is due to its smaller cultivation area but similar simulated production in CLM5 compared to FAO records.

**Decompose climate effects per crop type**

We established multiple linear regression (MLR) for each 0.9° × 1.25° grid cell and each crop type to determine how SG or ER-induced changes in different climate variables contribute to yield change with reference to RCP85 during the intervention period 2020-2099:

$$\log(Y_i) - \log(Y_c) = \beta_0 + \beta_i(X_i - X_c) + \varepsilon \quad (1)$$

where $Y$ is the CLM5 modelled yield, $\beta$ is a vector of coefficients ($\beta_0$ for the intercept) and $X$ is a vector of explanatory variables including surface air temperature (T), direct solar (RD) and diffuse (RI) radiation, precipitation (P) and relative humidity (RH), all growing season means based on each crop's planting dates. $\varepsilon$ is the residual error for any factors not captured by the explanatory variables. Subscript $i$ indicates one of the SGs (SAI, MSB, CCT) or ER ($RCP45_{(SSP5LU)}$) simulations, and $c$ indicates the control simulation, which is RCP85 for the SGs but $RCP85_{(45CO2)}$ for the ER, such that all scenarios have the same land use and $CO_2$ pathways in order to decompose climate-only effects. We focused on the transient effects of changes in climate due to SG or ER on yield in relative terms, ($\log(Y_i) - \log(Y_c) = \log(\frac{Y_i}{Y_c})$, because yields follow a log-normal distribution[54]. In this way, our statistical analyses focused on relative impacts of per unit changes in climate variables on each crop no matter what the base yields are across grid cells and regions. We tested the sensitivity of irrigated crops to P and RH and found no significant effects, because irrigated crops receive adequate water to reduce water stress every day in the CLM5 (applying unlimited water to offset soil moisture deficit of the irrigated crop columns at 6 AM local time). Thus, for irrigated crops, the terms for moisture (P, RH) were excluded from the regression.

We conducted the MLR for each crop using Eq. (1) at each grid cell if the specific crop's cultivation area exceeds 1000 hectare in that cell for more than 60 years between 2020 and 2099 (i.e., 6641 unique grid cells contributing to 23928 crop-grid specific regressions, with each MLR based on a one-dimensional time series of $60 \leq n \leq 80$). Although land use data are identical between the experimental (*i*) and control (*c*) simulations, due to crop distribution changes across years, some grid cells that do not meet the above criteria were excluded from the MLR for each specific crop. Grid cells with crop failures (zero or small yield values) in some years were set with a minimal yield for each crop type according to its 5$^{th}$ global percentile. Average crop failure rate was 3.5% for RCP85, 3.7% for RCP45, 3.5% for SAI, 3.5% for MSB, and 3.4% for CCT. Setting a minimal yield was not only meant to ensure valid values of log(yield) but also to include crop failure related to extreme events. We checked the variance inflation factor (VIF) for multicollinearity among independent variables. The majority of grid-cell level MLRs (98%) had VIF < 10 (low multicollinearity) for all independent variables. Removing the 2% grid cells with VIF >10 did not affect the predicted relative contribution of partial climate effects but would slightly bias the MLR-predicted total effect compared to the original CLM5 modelled global average yield change. Thus, all the grid-cell level regressions were included in the final analysis. We tested interaction effects between T and RH and between RH and P in the MLR. The Akaike's 'An Information Criterion' (AIC) score showed only one interaction term between T and RH improved the model fit slightly but only significantly for sugarcane under SAI (see Extended Data Fig. 4). RH and P had no obvious interaction effect. We also tested for nonlinearity using the generalized additive model (GAM) with cubic splines for T and RH which allow for estimation of flexible responses. The GAM predicted global partial and total effects did not improve over those of MLR (Supplementary Fig. 9).

**Isolate $CO_2$ effect for ER**

CLM5 simulates the enhancement effect of rising atmospheric $CO_2$ concentration on vegetation productivity through multiple $CO_2$-regulated processes in leaf photosynthesis for $C_3$ plants[55] and $C_4$ plants[56] and stomatal conductance[57]. In order to isolate and quantify $CO_2$ fertilization effect for different crops in CLM5, an idealized scenario $RCP85_{(45CO2)}$ was designed which could represent a global warming scenario caused by greenhouse gases

other than $CO_2$ that do not fertilize the vegetation growth (such as methane), while $CO_2$ emission is restrained or reduced. Through regression analysis based on RCP85 − $RCP85_{(45CO2)}$, the $CO_2$ fertilization effect is largely linear and exhibits a tendency of acclimation when $CO_2$ level is high (Extended Data Fig. 3). Thus, both linear and quadratic terms were used for $CO_2$ in the regression. The quadratic function estimates a hyperbolic response of crop yield to $CO_2$ enrichment, consistent with findings from FACE experiments[58]. The $CO_2$ regression coefficients for different crops were then compared with observations or other models (details in the main text).

The isolated climate-only effects (change in log yield based on $RCP45_{(SSP5LU)}$ − $RCP85_{(45CO2)}$) and the effect of reduced $CO_2$ effect under ER (change in log yield based on $RCP85_{(45CO2)}$ − RCP85) were then merged for each crop at each grid cell to estimate the total effect of ER (equivalent to $RCP45_{(SSP5LU)}$ − RCP85 in log scale). The partial and total effects of ER were then aggregated to regional or global average effects (and translation from log scale to percentage effect) with the following procedure.

**Resampling and aggregation**

After decomposing the climate effects for SGs, and climate and $CO_2$ effects for ER per grid cell and finding the their global or regional means, we took a Monte Carlo or Bootstrap approach (similar to Tai et al.[23]) to resampling 1000 times the statistical predictions of partial and total effects at all participating grid cells for each crop in order to estimate their probability distribution for a region or the globe in each year under each scenario. At each time of resampling, a weighted-average method was applied to aggregate the grid level log effects (individual and compound effects of T, RD, RI, P, and RH for SG or ER, and $CO_2$ for ER) per year to a region or the globe for each crop type using its crop area in each specific grid as the weight. The aggregated partial and total effects in natural log were then translated to percentage effects per crop. The mean and confidence interval of the individual effects of T, RD, RI, P and RH, their combinations (e.g., RD+RI for radiation, P+RH for moisture) and the total effect on each crop were estimated from the resampling. Note, taking a different procedure, for example, translating log to percent effect per grid cell before resampling and aggregation would bias the partial climate effects because $\exp(\sum \log\left(\frac{Y_i}{Y_c}\right)) \neq \sum \frac{Y_i}{Y_c}$.

To estimate global or regional average effects across all crop types, we weight-averaged the crop-specific percentage effects from the above steps using the product of crop area and base yield of each crop as the weight, which considers the significant variations in base yield, as well as plot size across samples of different crop types (Supplementary Fig. 1). The total effect on yield estimated from above statistical prediction of MLR, resampling, and aggregation steps was also compared with CLM modelled total effect (percentage change in global yield) under each SG (based on SAI/MSB/CCT – RCP85) or ER ($RCP45_{(SSP5LU)}$ – RCP85) to validate the statistical procedure. The difference between MLR estimated total effect and CLM5 modelled total effect indicates the residual errors (see Fig. 3 and Fig. 4). When land use change (LUC) effect was considered in the alternative ER scenario, the climate-only effects from MLR, $CO_2$ effect and LUC effect were summed (in log) at the grid-cell level followed by the same resampling and aggregation procedure to estimate the total effect for ER (see Information sections I and II, Supplementary Fig. 3).

Small variations exist in the effective radiative forcing across the SG methods (Table 1). After normalizing the effects of SGs using the scaling factors that match the mean and trend of top of atmosphere radiative flux imbalance reduction by each SG to that of ER (Supplementary Fig. 10-11), the temperature and total effects of CCT become stronger than those of SAI, MSB, and ER, but the overall advantage of SGs over ER and our main conclusions remain unchanged.

## Data availability

The intermediate data that support the findings of this study are available at https://doi.org/10.7910/DVN/Y1UHID. Source model data are available upon request from the corresponding author.

## Code availability

Code for replicating the figures and analysis is written in R (version 3.6.2) or NCAR Command Language Version 6.5.0 and has been deposited in the Harvard Dataverse https://doi.org/10.7910/DVN/Y1UHID.

NorESM1-ME is available at https://github.com/NorESMhub/NorESM. CLM5 is available at https://github.com/ESCOMP/CTSM.

## References


1. Lawrence, M. G. *et al.* Evaluating climate geoengineering proposals in the context of the Paris Agreement temperature goals. *Nature Communications* **9**, (2018).
2. MacMartin, D. G., Ricke, K. L. & Keith, D. W. Solar geoengineering as part of an overall strategy for meeting the 1.5°C Paris target. *Philosophical Transactions of the Royal Society A: Mathematical, Physical and Engineering Sciences* **376**, 20160454 (2018).
3. Crutzen, P. J. Albedo enhancement by stratospheric sulfur injections: A contribution to resolve a policy dilemma? *Climatic Change* **77**, 211–220 (2006).
4. Ahlm, L. *et al.* Marine cloud brightening – as effective without clouds. *Atmos. Chem. Phys.* **17**, 13071–13087 (2017).
5. Muri, H. *et al.* Climate response to aerosol geoengineering: A multimethod comparison. *J. Climate* **31**, 6319–6340 (2018).
6. Kravitz, B. *et al.* The Geoengineering Model Intercomparison Project (GeoMIP). *Atmospheric Science Letters* **12**, 162–167 (2011).
7. Robock, A., Oman, L. & Stenchikov, G. L. Regional climate responses to geoengineering with tropical and Arctic SO2 injections. *Journal of Geophysical Research: Atmospheres* **113**, (2008).
8. Tjiputra, J. F., Grini, A. & Lee, H. Impact of idealized future stratospheric aerosol injection on the large-scale ocean and land carbon cycles. *J. Geophys. Res. Biogeosci.* **121**, 2015JG003045 (2016).
9. Russell, L. M. *et al.* Ecosystem Impacts of Geoengineering: A Review for Developing a Science Plan. *Ambio* **41**, 350–369 (2012).
10. Xia, L. *et al.* Solar radiation management impacts on agriculture in China: A case study in the Geoengineering Model Intercomparison Project (GeoMIP). *Journal of Geophysical Research: Atmospheres* **119**, 8695–8711 (2014).
11. Zhan, P., Zhu, W., Zhang, T., Cui, X. & Li, N. Impacts of sulfate geoengineering on rice yield in china: Results from a multimodel ensemble. *Earth's Future* **7**, 395–410 (2019).

12. Parkes, B., Challinor, A. & Nicklin, K. Crop failure rates in a geoengineered climate: impact of climate change and marine cloud brightening. *Environmental Research Letters* **10**, 084003 (2015).
13. Yang, H. *et al.* Potential negative consequences of geoengineering on crop production: A study of Indian groundnut. *Geophysical Research Letters* **43**, (2016).
14. Pongratz, J., Lobell, D. B., Cao, L. & Caldeira, K. Crop yields in a geoengineered climate. *Nature Climate Change* **2**, 101–105 (2012).
15. Proctor, J., Hsiang, S., Burney, J., Burke, M. & Schlenker, W. Estimating global agricultural effects of geoengineering using volcanic eruptions. *Nature* **560**, 480 (2018).
16. Tjiputra, J. F. *et al.* Evaluation of the carbon cycle components in the Norwegian Earth System Model (NorESM). *Geoscientific Model Development* **6**, 301–325 (2013).
17. MacMartin, D. G. & Kravitz, B. Mission-driven research for stratospheric aerosol geoengineering. *PNAS* **116**, 1089–1094 (2019).
18. Lombardozzi, D. L. *et al.* Simulating agriculture in the Community Land Model Version 5. *Journal of Geophysical Research: Biogeosciences* **125**, e2019JG005529 (2020).
19. Popp, A. *et al.* Land-use futures in the shared socio-economic pathways. *Global Environmental Change* **42**, 331–345 (2017).
20. O'Neill, B. C. *et al.* The Scenario Model Intercomparison Project (ScenarioMIP) for CMIP6. *Geoscientific Model Development* **9**, 3461–3482 (2016).
21. IPCC. *Climate Change 2013: The Physical Science Basis: Working Group I Contribution to the Fifth Assessment Report of the Intergovernmental Panel on Climate Change [Stocker, T.F., D. Qin, G.-K. Plattner, M. Tignor, S.K. Allen, J. Boschung, A. Nauels, Y. Xia, V. Bex and P.M. Midgley (eds.)]*. (Cambridge University Press, 2013).
22. Food and Agriculture Organization of the United Nations. FAOSTAT statistics database. http://www.fao.org/faostat/en/?#data/QC (2019).
23. Tai, A. P. K., Martin, M. V. & Heald, C. L. Threat to future global food security from climate change and ozone air pollution. *Nature Clim Change* **4**, 817–821 (2014).

24. Hsiao, J., Swann, A. L. S. & Kim, S.-H. Maize yield under a changing climate: The hidden role of vapor pressure deficit. *Agricultural and Forest Meteorology* **279**, 107692 (2019).
25. Grossiord, C. *et al.* Plant responses to rising vapor pressure deficit. *New Phytologist* (2020) doi:10.1111/nph.16485.
26. Rigden, A. J., Mueller, N. D., Holbrook, N. M., Pillai, N. & Huybers, P. Combined influence of soil moisture and atmospheric evaporative demand is important for accurately predicting US maize yields. *Nature Food* **1**, 127–133 (2020).
27. Konings, A. G., Williams, A. P. & Gentine, P. Sensitivity of grassland productivity to aridity controlled by stomatal and xylem regulation. *Nature Geoscience* **10**, 284–288 (2017).
28. Novick, K. A. *et al.* The increasing importance of atmospheric demand for ecosystem water and carbon fluxes. *Nature Climate Change* **6**, 1023–1027 (2016).
29. Ainsworth, E. A. & Long, S. P. What have we learned from 15 years of free-air CO2 enrichment (FACE)? A meta-analytic review of the responses of photosynthesis, canopy properties and plant production to rising CO2: Tansley review. *New Phytologist* **165**, 351–372 (2004).
30. Bishop, K. A., Leakey, A. D. B. & Ainsworth, E. A. How seasonal temperature or water inputs affect the relative response of $C_3$ crops to elevated $CO_2$: a global analysis of open top chamber and free air $CO_2$ enrichment studies. *Food and Energy Security* **3**, 33–45 (2014).
31. Ainsworth, E. A. *et al.* A meta-analysis of elevated $CO_2$ effects on soybean (Glycine max) physiology, growth and yield. *Global Change Biology* **8**, 695–709 (2002).
32. Leakey, A. D. B. Rising atmospheric carbon dioxide concentration and the future of $C_4$ crops for food and fuel. *Proceedings of the Royal Society B: Biological Sciences* **276**, 2333–2343 (2009).
33. Ainsworth, E. A. & Rogers, A. The response of photosynthesis and stomatal conductance to rising $CO_2$: mechanisms and environmental interactions. *Plant, Cell & Environment* **30**, 258–270 (2007).
34. National Research Council. *Climate Intervention: Reflecting Sunlight to Cool Earth*. (National Academies Press, 2015). doi:10.17226/18988.

35. Lutsko, N. J., Seeley, J. T. & Keith, D. W. Estimating impacts and trade-offs in solar geoengineering scenarios with a moist energy balance model. *Geophysical Research Letters* **47**, e2020GL087290 (2020).
36. Friedlingstein, P. *et al.* Uncertainties in CMIP5 climate projections due to carbon cycle feedbacks. *J. Climate* **27**, 511–526 (2014).
37. Tilmes, S. *et al.* The hydrological impact of geoengineering in the Geoengineering Model Intercomparison Project (GeoMIP). *Journal of Geophysical Research: Atmospheres* **118**, 11,036-11,058 (2013).
38. Lawrence, D. M. *et al.* The Community Land Model Version 5: Description of new features, benchmarking, and impact of forcing uncertainty. *Journal of Advances in Modeling Earth Systems* **11**, 4245–4287 (2019).
39. Fisher, R. A. *et al.* Parametric controls on vegetation responses to biogeochemical forcing in the CLM5. *Journal of Advances in Modeling Earth Systems* **11**, 2879–2895 (2019).
40. Bonan, G. B. *et al.* Model structure and climate data uncertainty in historical simulations of the terrestrial carbon cycle (1850–2014). *Global Biogeochemical Cycles* **33**, 1310–1326 (2019).
41. Osborne, T., Rose, G. & Wheeler, T. Variation in the global-scale impacts of climate change on crop productivity due to climate model uncertainty and adaptation. *Agricultural and Forest Meteorology* **170**, 183–194 (2013).
42. Peng, B. *et al.* Improving maize growth processes in the community land model: Implementation and evaluation. *Agricultural and Forest Meteorology* **250–251**, 64–89 (2018).
43. Buzan, J. R. & Huber, M. Moist Heat Stress on a Hotter Earth. *Annu. Rev. Earth Planet. Sci.* **48**, 623–655 (2020).
44. Wieder, W. R. *et al.* Beyond static benchmarking: Using experimental manipulations to evaluate land model assumptions. *Global Biogeochemical Cycles* **33**, 1289–1309 (2019).
45. Mercado, L. M. *et al.* Impact of changes in diffuse radiation on the global land carbon sink. *Nature* **458**, 1014–1017 (2009).
46. Cheng, S. J. *et al.* Variations in the influence of diffuse light on gross primary productivity in temperate ecosystems. *Agricultural and Forest Meteorology* **201**, 98–110 (2015).

47. Shao, L. *et al.* The fertilization effect of global dimming on crop yields is not attributed to an improved light interception. *Global Change Biology* **26**, 1697–1713 (2020).
48. Vattioni, S. *et al.* Exploring accumulation-mode $H_2SO_4$ versus $SO_2$ stratospheric sulfate geoengineering in a sectional aerosol–chemistry–climate model. *Atmospheric Chemistry and Physics* **19**, 4877–4897 (2019).
49. Levis, S., Badger, A., Drewniak, B., Nevison, C. & Ren, X. CLMcrop yields and water requirements: avoided impacts by choosing RCP 4.5 over 8.5. *Climatic Change* **146**, 501–515 (2018).
50. Fricko, O. *et al.* The marker quantification of the Shared Socioeconomic Pathway 2: A middle-of-the-road scenario for the 21st century. *Global Environmental Change* **42**, 251–267 (2017).
51. Lauvset, S. K., Tjiputra, J. & Muri, H. Climate engineering and the ocean: effects on biogeochemistry and primary production. *Biogeosciences* **14**, 5675–5691 (2017).
52. Hurtt, G. C. *et al.* Harmonization of land-use scenarios for the period 1500–2100: 600 years of global gridded annual land-use transitions, wood harvest, and resulting secondary lands. *Climatic Change* **109**, 117–161 (2011).
53. West, T. O. *et al.* Cropland carbon fluxes in the United States: increasing geospatial resolution of inventory-based carbon accounting. *Ecological Applications* **20**, 1074–1086 (2010).
54. Lobell, D. B., Schlenker, W. & Costa-Roberts, J. Climate trends and global crop production since 1980. *Science* **333**, 616–620 (2011).
55. Farquhar, G., von Caemmerer, S. von & Berry, J. A biochemical model of photosynthetic CO2 assimilation in leaves of C3 species. *Planta* **149**, 78–90 (1980).
56. Collatz, G. J., Ribas-Carbo, M. & Berry, J. A. Coupled photosynthesis-stomatal conductance model for leaves of $C_4$ plants. *Functional Plant Biol.* **19**, 519–538 (1992).
57. Medlyn, B. E. *et al.* Reconciling the optimal and empirical approaches to modelling stomatal conductance. *Global Change Biology* **17**, 2134–2144 (2011).
58. Long, S. P., Ainsworth, E. A., Leakey, A. D. B., Nösberger, J. & Ort, D. R. Food for thought: lower-than-expected crop yield stimulation with rising $CO_2$ concentrations. *Science* **312**, 1918–1921 (2006).

## Acknowledgements

This study was supported by the Bjerknes Centre for Climate Research SKD-Fast Track Initiatives project (808011) and by Harvard University's Solar Geoengineering Research Program fellowship. JT was supported by the Research Council of Norway funded projects INES (270061) and COLUMBIA (275268). Y.F. and J.T. acknowledge funding from the European Commission, H2020 framework program (CRESCENDO, no 641816). C.-E. P. was supported by Brain Pool Programs through the National Research Foundation of Korea (NRF) funded by the Ministry of Science and ICT (2019H1D3A1A01071022). The simulations were performed on resources provided by UNINETT Sigma2 –the National Infrastructure for High Performance Computing and Data Storage in Norway, account NS2345K and NS9033K. A. Grini provided original SAI experimental settings in NorESM1-ME and P. Lawrence provided surface input data for CLM5. The authors also thank P. Irvine, J. Proctor, K. McColl and A. Berg for their helpful comments and communications on this work.

## Author contributions

Y.F. and J.T. designed the study; Y.F. conducted the simulations and analysed the data with contributions from J.T., H.M. and D.L.; H.M. provided original MSB and CCT experimental settings; Y.F., J.T., H.M., D.L., C.-E.P., S.W. and D.K. interpreted the data and results; Y.F. wrote the first draft and all authors contributed to editing and revising the manuscript.

## Competing interests

The authors declare no competing interests.

## Supplementary information

The Supplementary Information file includes text sections I and II, Supplementary Table 1, and Supplementary Figures 1-11.

## Figure Legends

**Fig. 1: Methodology and global summary of key model variables. a**, Experimental design of SGs and ER as alternative pathways to offsetting the anthropogenic radiative forcing from RCP85 down to RCP45, climate simulations from NorESM1-ME are used to force CLM5 crop simulations and steps to quantify the partial and total climate effects by multiple linear regression (MLR) and to isolate $CO_2$ effect for ER (see Methods for details). **b**, The left and right panels depict the temperature time-series (5-year running mean) of global annual mean over all land surface and the growing season mean over

crop-area only. Dashed lines are respective preindustrial (1850-1879 mean) values. **c-f**, Time-series (5-year running mean) of global crop-area weighted average direct and diffuse solar radiation (visible band 0.3-0.7$\mu$m only; **c**), precipitation and relative humidity (**d**) simulated by NorESM1-ME, annual total crop area, nitrogen fertilization and irrigation fraction under two land use pathways SSP2 and SSP5 (**e**) and CLM5 simulated annual global crop yield (**f**) in different experiments shown in Table 1.

**Fig. 2: Validation of CLM simulated crop production and yield for the recent past with FAO data**. **a**, Comparison of annual production (black) and cultivation area (orange) of six crops between CLM5 (dashed) and FAO observations (solid) for the period 2006-2018. **b**, Model-data comparison on per hectare yield.

**Fig. 3: Partial and total effects of SG or ER on global crop yield**. **a-d**, Time series (5-year running mean) of partial climate (T-temperature, RD-direct radiation, RI-diffuse radiation, P-precipitation, RH-relative humidity) effects decomposed by MLR analysis, the isolated $CO_2$ effect for ER, MLR predicted and CLM5 modelled total effects under SAI (**a**), MSB (**b**), CCT (**c**) and ER-emissions reduction ($RCP45_{(SSP5LU)}$; **d**) relative to RCP85 in the 21$^{st}$ century. $CO_2$ effect is not shown (irrelevant for SG) in **a-c**. Lines indicate the mean effects and error bars indicate the 2.5$^{th}$ to 97.5$^{th}$ percentile confidence interval for MLR predictions (the CLM5 modelled total effect and $CO_2$ effect only show the means). **e**, Boxplot of mean partial and total effects for the period of 2075-2099 (the lower and upper hinges of the box, the horizontal line in the box, and the ends of whiskers indicate the first and third quartiles, the median, and the smallest and largest values within 1.5 times the inter-quartile range from the hinges, respectively. Points beyond the end of the whiskers are outliers). Global yield is crop-area weighted average across six crop types. The difference between MLR estimated total effect and CLM5 modelled total effect indicates the residual errors (average -0.8%, 1.1%, 0.3%, -0.6% for the SAI, MSB, CCT and ER scenarios, respectively, during 2075-2099).

**Fig. 4: Global partial and total effects of SG or ER on yield per crop type. a**, Rainfed crops consider all climate variables (abbreviations as in Fig. 3) and $CO_2$ (for ER) relative to RCP85. **b**, Irrigated crops ignore moisture related variables P and RH (see Methods). Error bars indicate the 2.5$^{th}$ to 97.5$^{th}$ percentile confidence interval averaged over the period of 2075-2099. Note the y-axis ranges of irrigated (**b**) are only half of those of rainfed (**a**), suggesting much weaker sensitivity of irrigated crops. The difference between MLR estimated total effect and CLM5 modelled total effect indicates the residual errors (-1.0%, -3%, -1.8%, 0.6%, 1.0% and 4.0% for rainfed, and -1.5%, 0.1%, 0.1%, -0.04%, -0.4% and 0.1% for irrigated maize, sugarcane, wheat, rice, soy and cotton, respectively, average across the scenarios during 2075-2099).

559 **Fig. 5**: **CLM5 simulated change in global crop yield under SG or ER**. **a-d**, Absolute changes in yield under SAI (**a**), MSB
560 (**b**), CCT (**c**) and ER ($RCP45_{(SSP5LU)}$; **d**) compared to RCP85 (2075-2099 mean; tonnes $ha^{-1}$). The six region boxes indicate
561 North America (NAM), Central America (CAM), South America (SAM), Europe and Western Asia (EUA), Southeast Asia
562 (SEA), Central and Southern Africa (SAF).

## Tables

**Table 1**: Description of experimental set-up including land use, radiative forcing, $CO_2$ concentration under different climate scenarios used as input for crop simulations. All values depict global average.

| Case name | Climate | Land use | Radiative forcing | | $CO_2$ | Note |
|---|---|---|---|---|---|---|
| | | | Effective radiative forcing by 2100 [W $m^{-2}$] | Shortwave radiation [2090-2099; W $m^{-2}$] | Atmospheric $CO_2$ concentration [2020 to 2100; ppm] | |
| **RCP45** | RCP4.5 | SSP2 | 4.5 (−4) | 187.8 | 409-538 | Original RCP45 |
| **RCP45$_{(SSP5LU)}$** | RCP4.5 | SSP5 | 4.5 (−4) | 187.8 | 409-538 | RCP45 climate with SSP5 land use to represent ER compared to RCP85 |
| **RCP85** | RCP8.5 | SSP5 | 8.5 | 187.6 | 413-936 | Default RCP85 |
| **RCP85$_{(45CO2)}$** | RCP8.5 | SSP5 | 8.5 | 187.6 | 409-538 | RCP85 climate with RCP45 $CO_2$ to isolate $CO_2$ effect |
| **SAI** | RCP8.5+ SAI | SSP5 | 4.5 (−4) | 182.7 | 413-936 | Same $CO_2$ as in RCP85 |
| **MSB** | RCP8.5+ MSB | SSP5 | 4.5 (−4) | 186.5 | 413-936 | Same $CO_2$ as in RCP85 |
| **CCT** | RCP8.5+ CCT | SSP5 | 4.7 (−3.8) | 192.7 | 413-936 | Same $CO_2$ as in RCP85 |

RCP45$_{(SSP5LU)}$ is intended to compare with the original RCP45 to isolate potential effects related to changing land use. It also allows to focus on ER-emissions reduction (climate and $CO_2$ effects) when compared to RCP85. Experiment RCP85$_{(45CO2)}$ is representative of a global warming scenario caused by non-$CO_2$ greenhouse gases (e.g., methane) for comparison with RCP85 to isolate $CO_2$ fertilization effect. Values in parentheses of column 3 are the net radiative forcing compared to RCP85 by the end of the twenty first century. CCT has a maximum achievable radiative forcing of −3.8 W $m^{-2}$ in NorESM1-ME[5], slightly lower than SAI and MSB. SAI, MSB and CCT were designed to reduce the radiative forcing of the concentration-driven RCP85 scenario to the level of RCP45 through SG techniques, but the original SG experiments used the emission-driven NorESM1-ME, which simulated slightly larger difference in radiative forcing between RCP85 and RCP45 than their concentration-driven counterparts due to carbon cycle feedbacks[5]. Here in CLM5 offline simulations, the same input $CO_2$ levels are prescribed for SAI, MSB and CCT according to the concentration driven RCP85, because the difference in atmospheric $CO_2$ is relatively small.

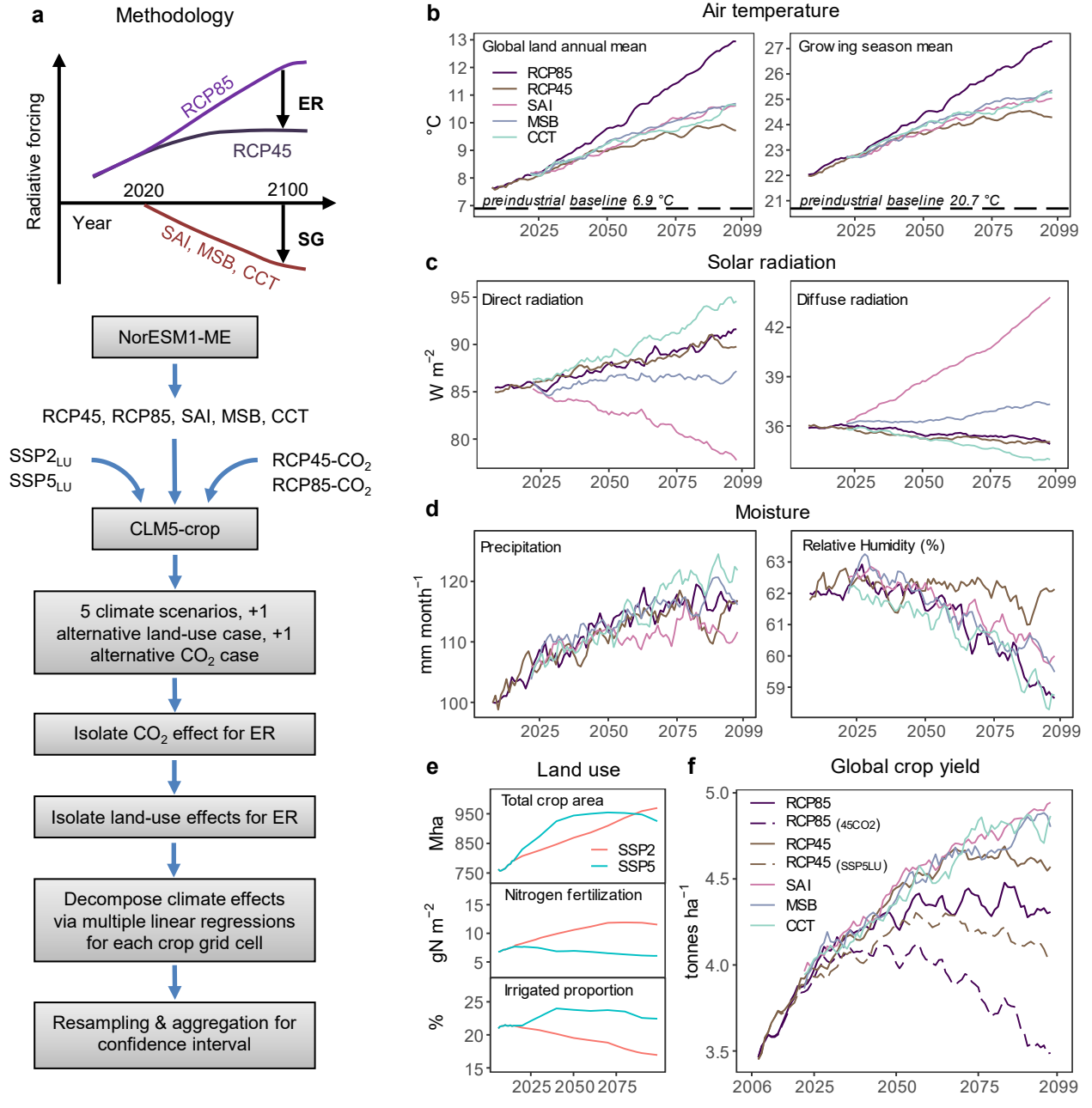
a
Methodology
Radiative forcing
RCP85
RCP45
ER
2020
2100
Year
SAI, MSB, CCT
SG
NorESM1-ME
RCP45, RCP85, SAI, MSB, CCT
SSP2LU
SSP5LU
RCP45-CO2
RCP85-CO2
CLM5-crop
5 climate scenarios, +1 alternative land-use case, +1 alternative CO2 case
Isolate CO2 effect for ER
Isolate land-use effects for ER
Decompose climate effects via multiple linear regressions for each crop grid cell
Resampling & aggregation for confidence interval
b
Air temperature
Global land annual mean
RCP85
RCP45
SAI
MSB
CCT
°C
preindustrial baseline 6.9 °C
Growing season mean
preindustrial baseline 20.7 °C
c
Solar radiation
Direct radiation
W m−2
Diffuse radiation
d
Moisture
Precipitation
mm month−1
Relative Humidity (%)
e
Land use
Total crop area
Mha
SSP2
SSP5
Nitrogen fertilization
gN m−2
Irrigated proportion
%
f
Global crop yield
RCP85
RCP85 (45CO2)
RCP45
RCP45 (SSP5LU)
SAI
MSB
CCT
tonnes ha−1

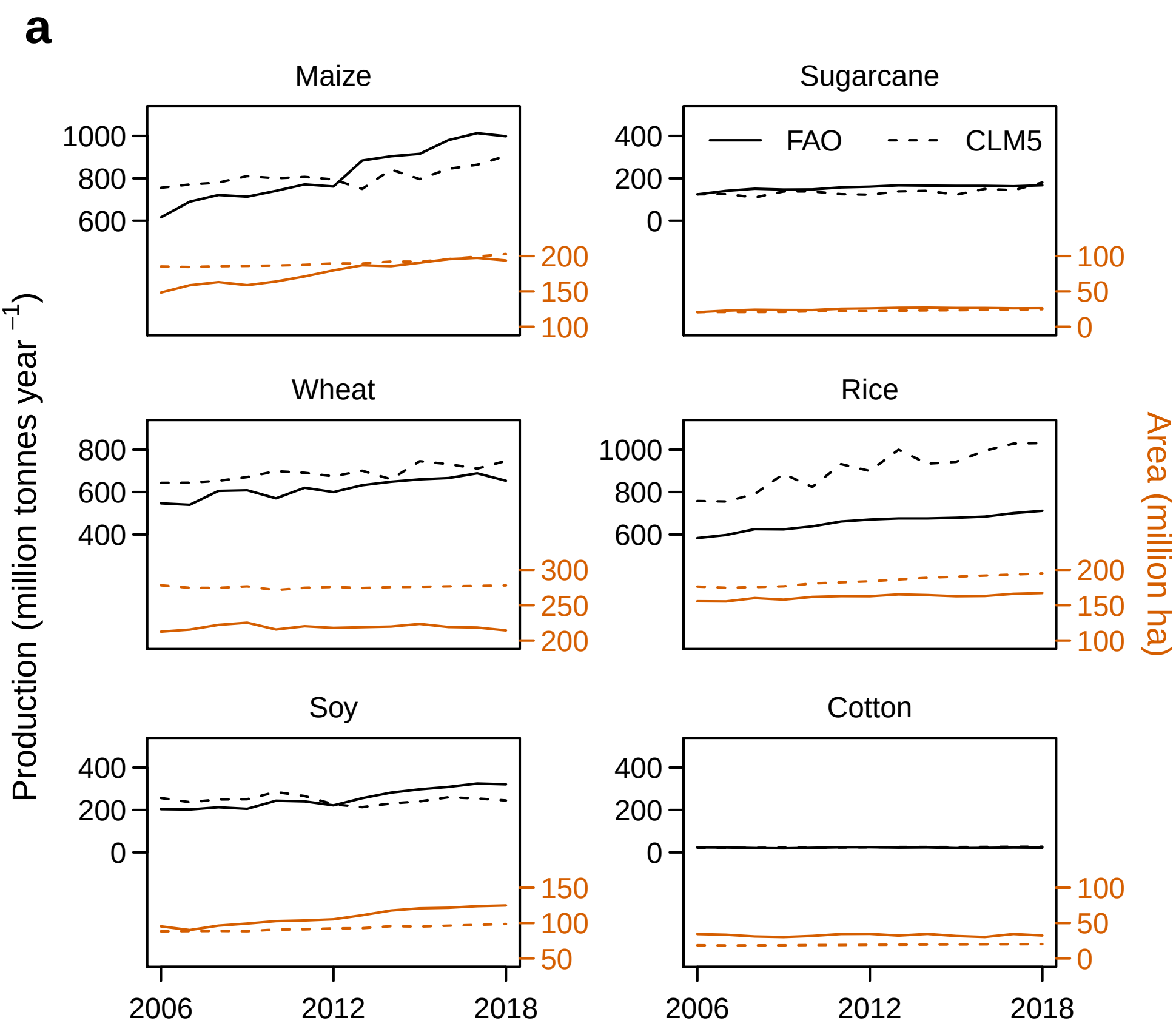
a
Maize
Sugarcane
Wheat
Rice
Soy
Cotton
FAO
CLM5
Production (million tonnes year −1)
Area (million ha)
1000
800
600
400
200
0
100
50
150
250
300
2006
2012
2018

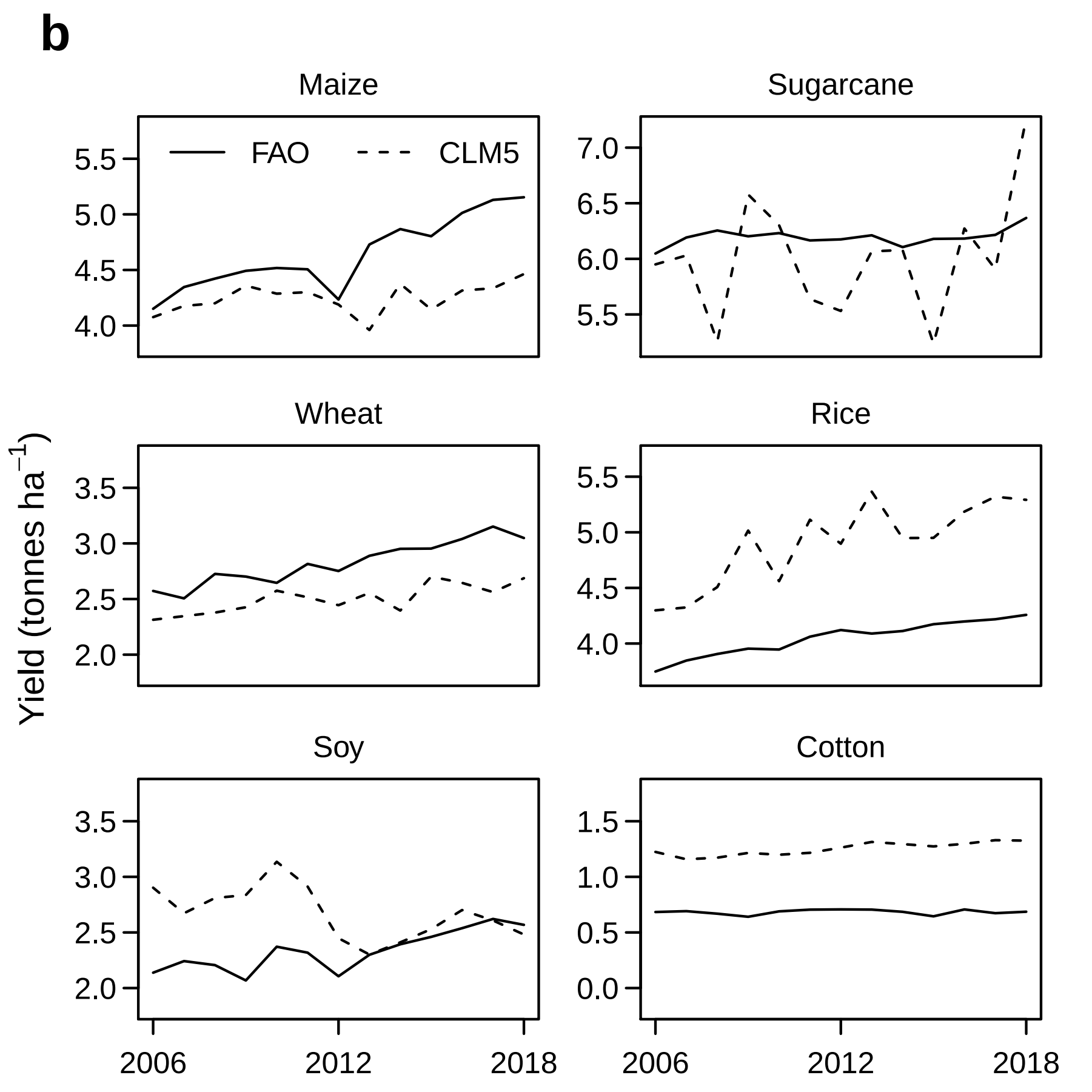
b
Maize
Sugarcane
Wheat
Rice
Soy
Cotton
FAO
CLM5
Yield (tonnes ha$^{-1}$)
5.5
5.0
4.5
4.0
7.0
6.5
6.0
5.5
3.5
3.0
2.5
2.0
5.5
5.0
4.5
4.0
3.5
3.0
2.5
2.0
1.5
1.0
0.5
0.0
2006
2012
2018
2006
2012
2018

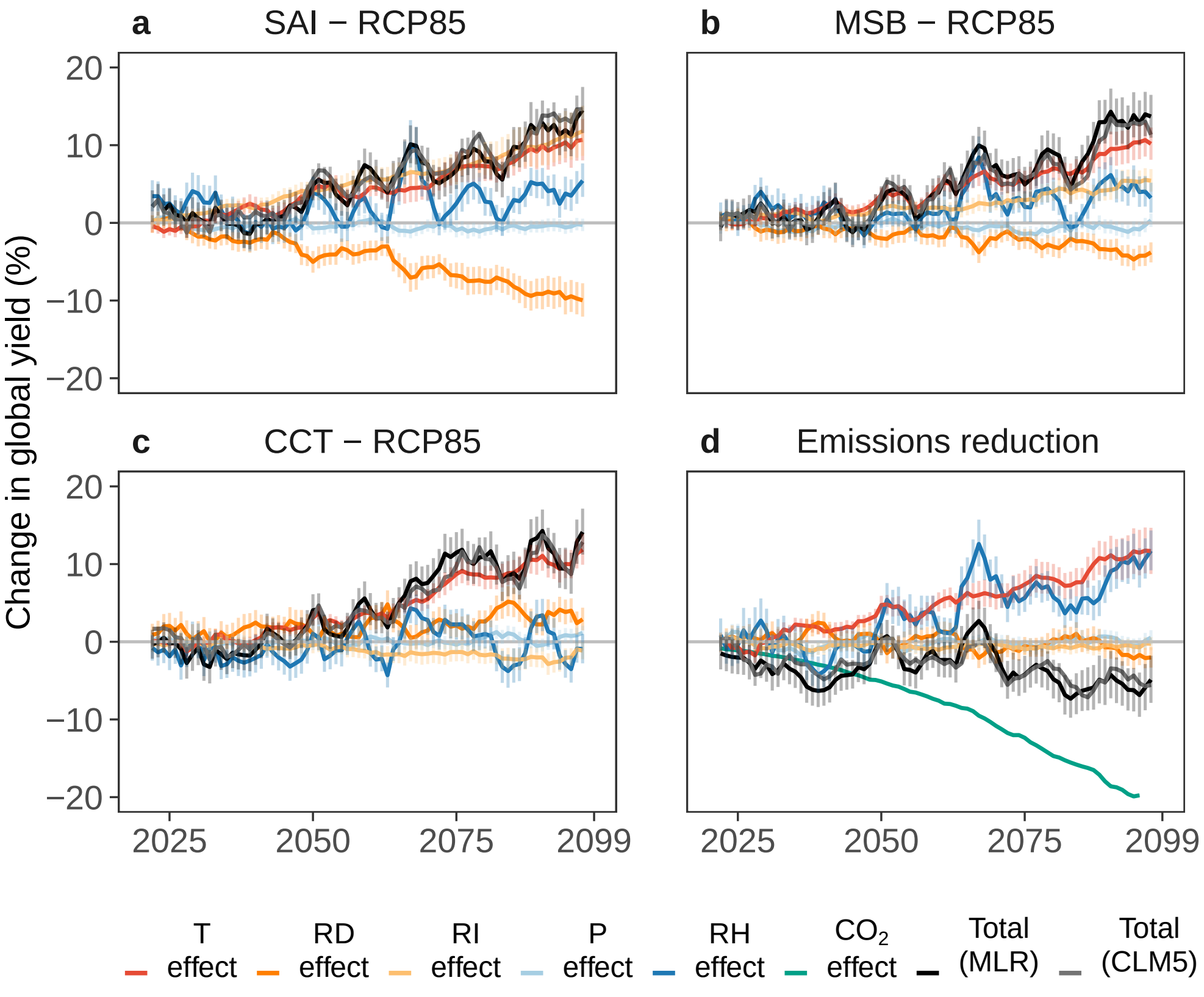
a
SAI − RCP85
b
MSB − RCP85
c
CCT − RCP85
d
Emissions reduction
Change in global yield (%)
20
10
0
−10
−20
2025
2050
2075
2099
T effect
RD effect
RI effect
P effect
RH effect
CO2 effect
Total (MLR)
Total (CLM5)

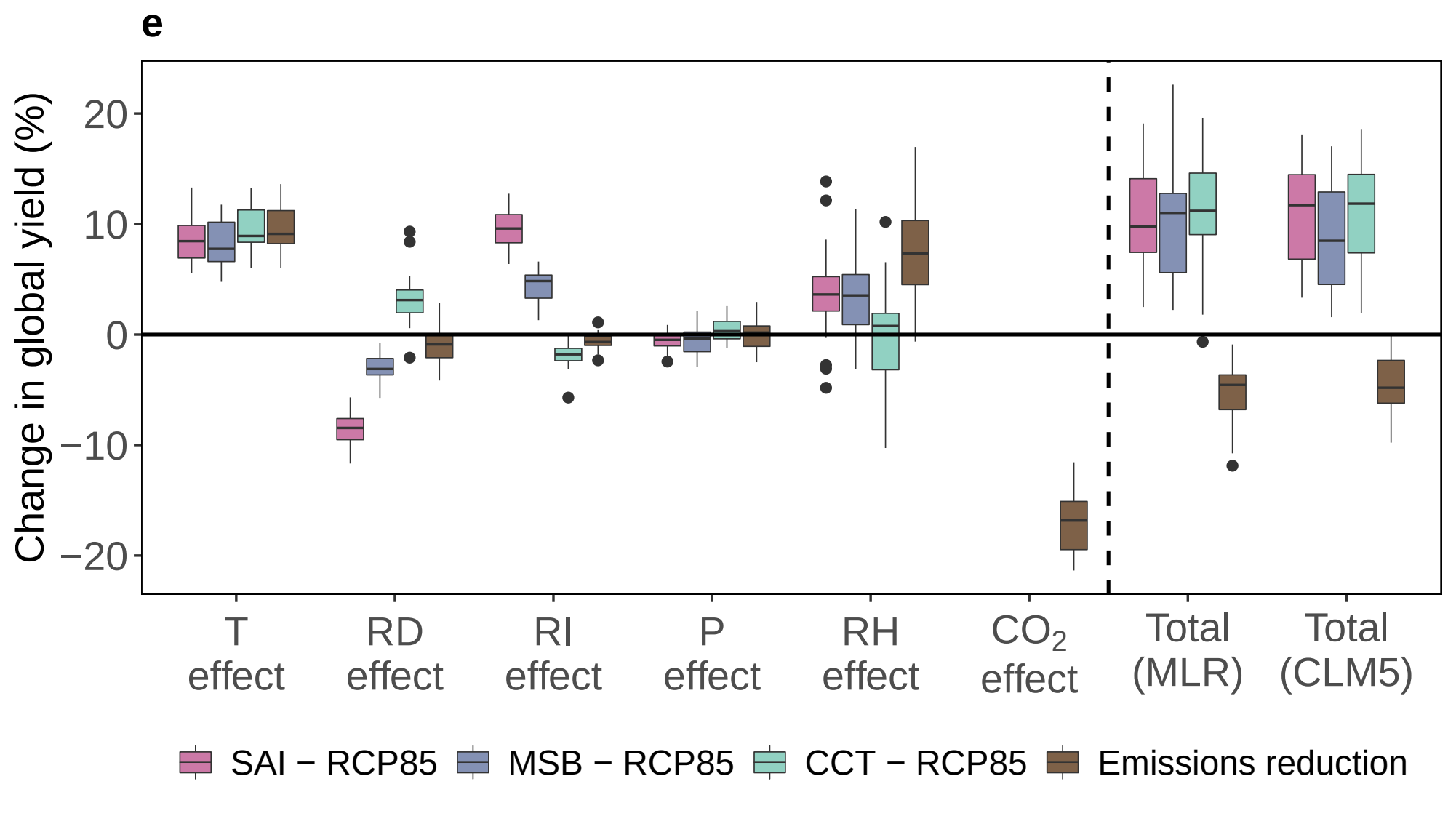
e
Change in global yield (%)
20
10
0
−10
−20
T effect
RD effect
RI effect
P effect
RH effect
$CO_2$ effect
Total (MLR)
Total (CLM5)
SAI − RCP85
MSB − RCP85
CCT − RCP85
Emissions reduction

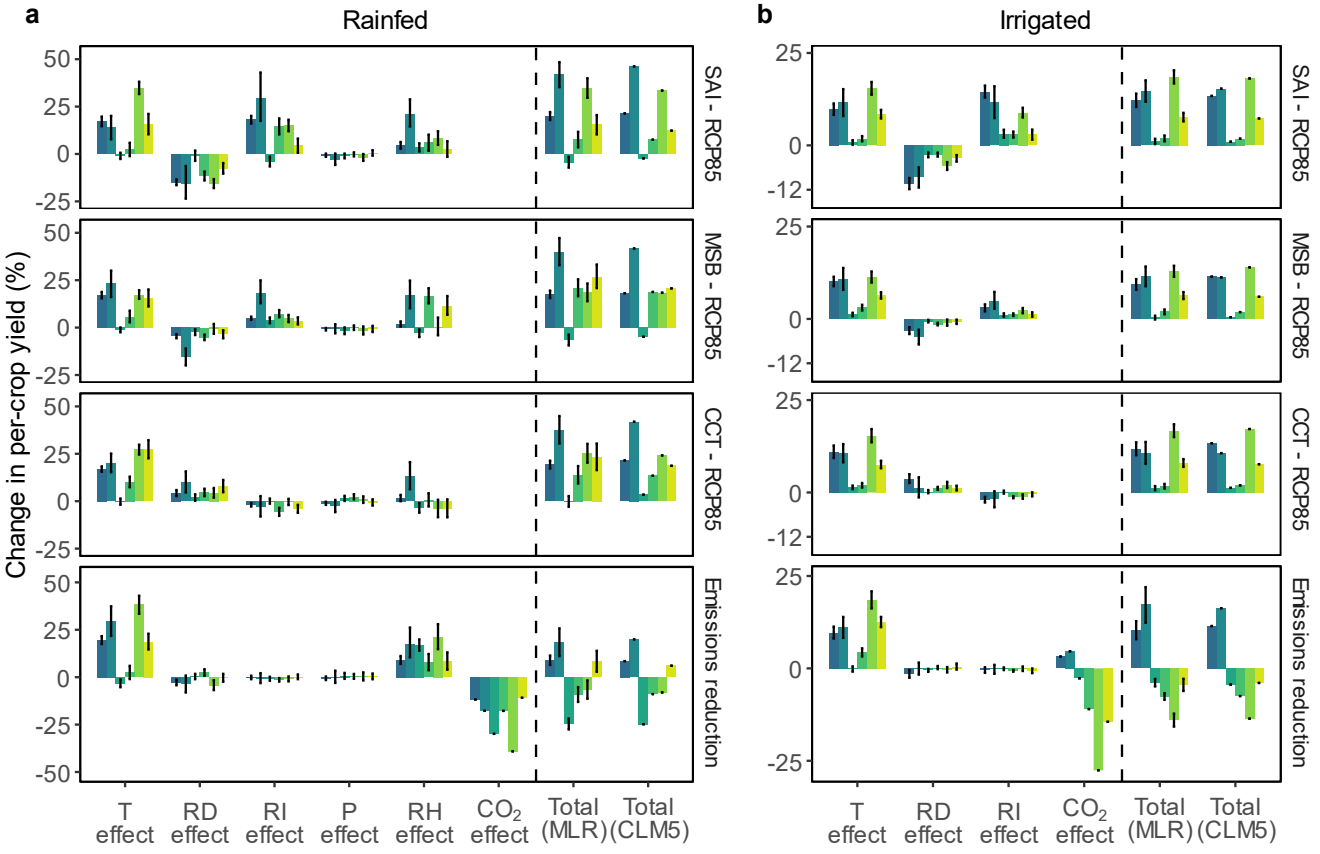
a
Rainfed
b
Irrigated
Change in per-crop yield (%)
SAI - RCP85
MSB - RCP85
CCT - RCP85
Emissions reduction
T effect
RD effect
RI effect
P effect
RH effect
CO2 effect
Total (MLR)
Total (CLM5)
Maize
Sugarcane
Wheat
Rice
Soy
Cotton

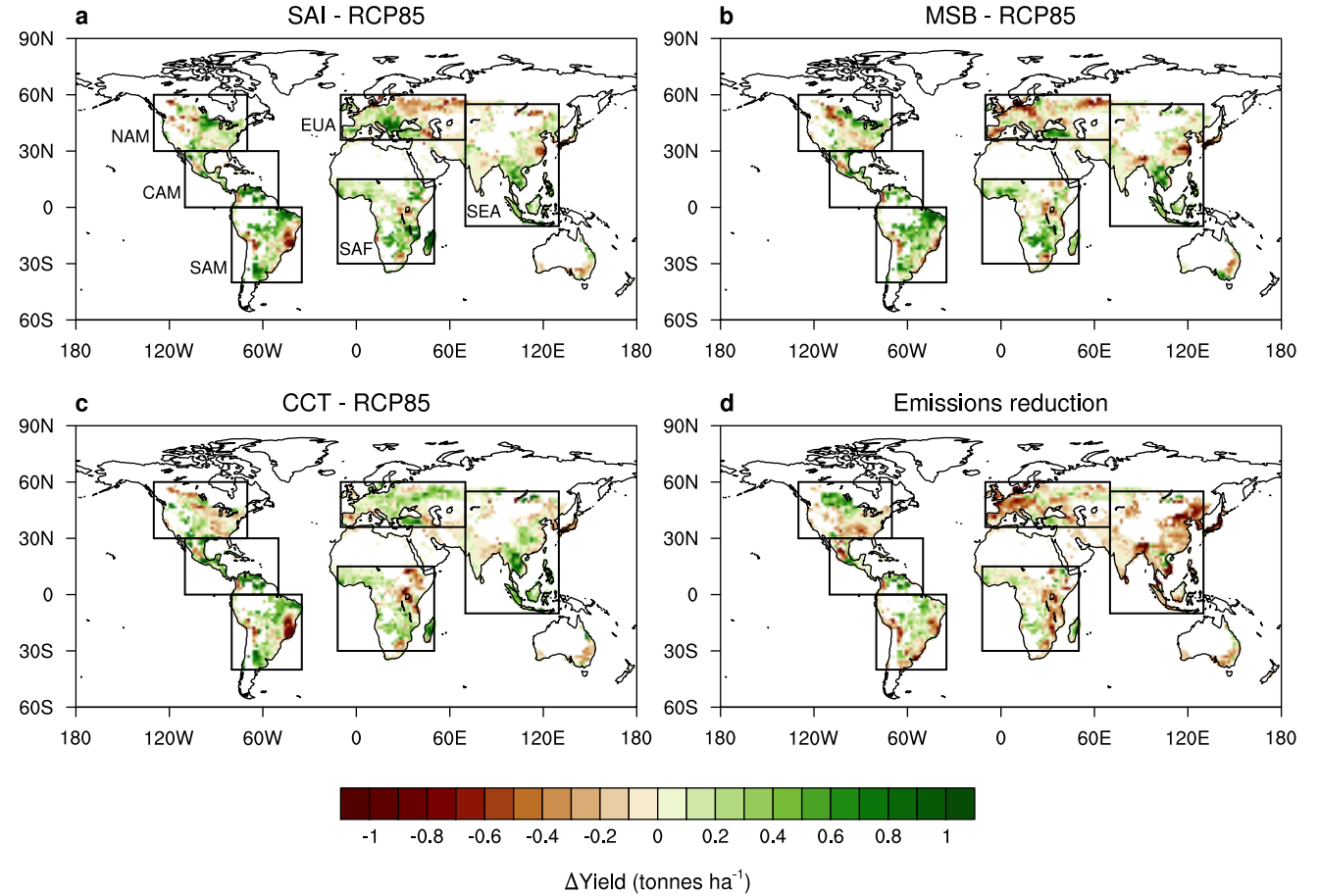
a
SAI - RCP85
b
MSB - RCP85
c
CCT - RCP85
d
Emissions reduction
NAM
EUA
CAM
SEA
SAF
SAM
90N
60N
30N
0
30S
60S
180
120W
60W
0
60E
120E
180
-1
-0.8
-0.6
-0.4
-0.2
0
0.2
0.4
0.6
0.8
1
ΔYield (tonnes ha-1)

**a** SAI - RCP85

**b** MSB - RCP85

**c** CCT - RCP85

**d** Emissions reduction

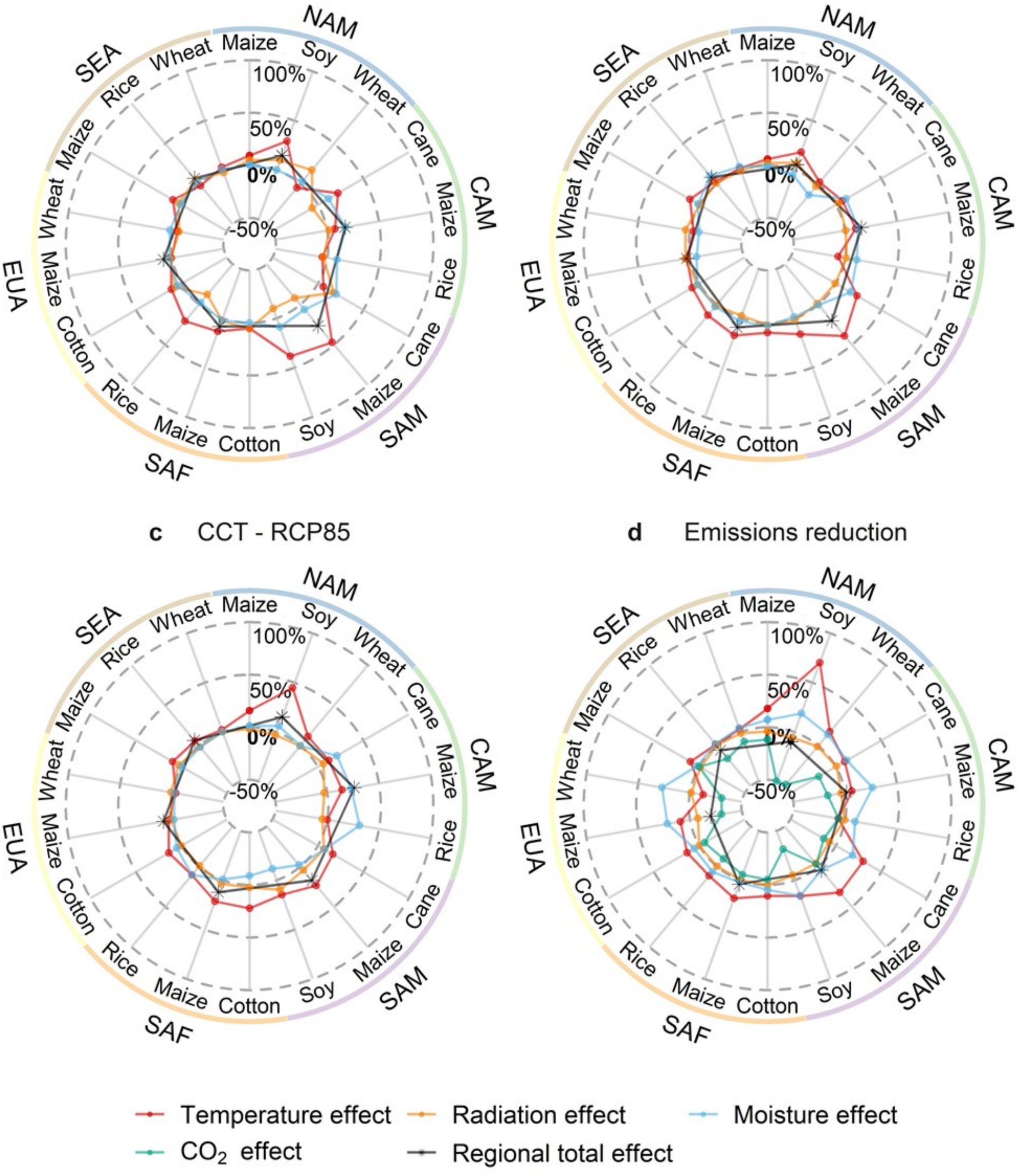

**a** SAI - RCP85

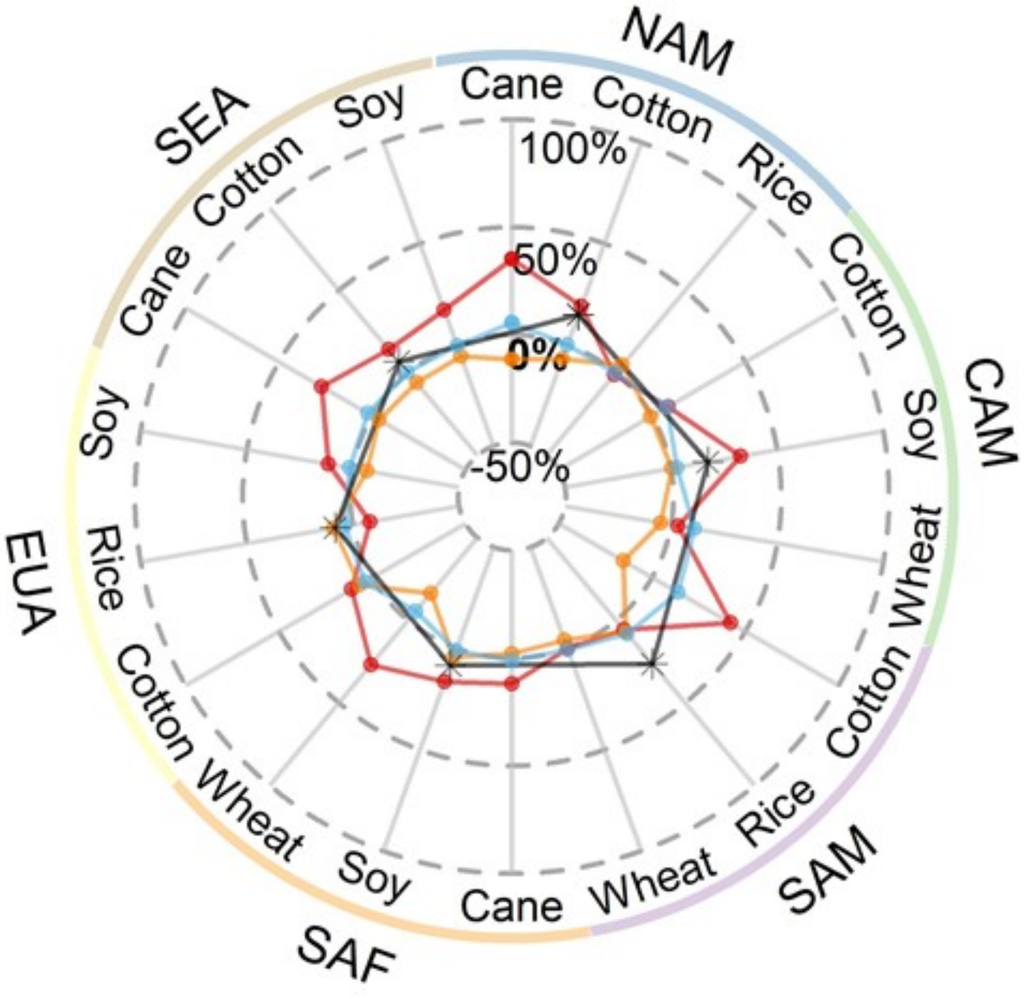


**b** MSB - RCP85

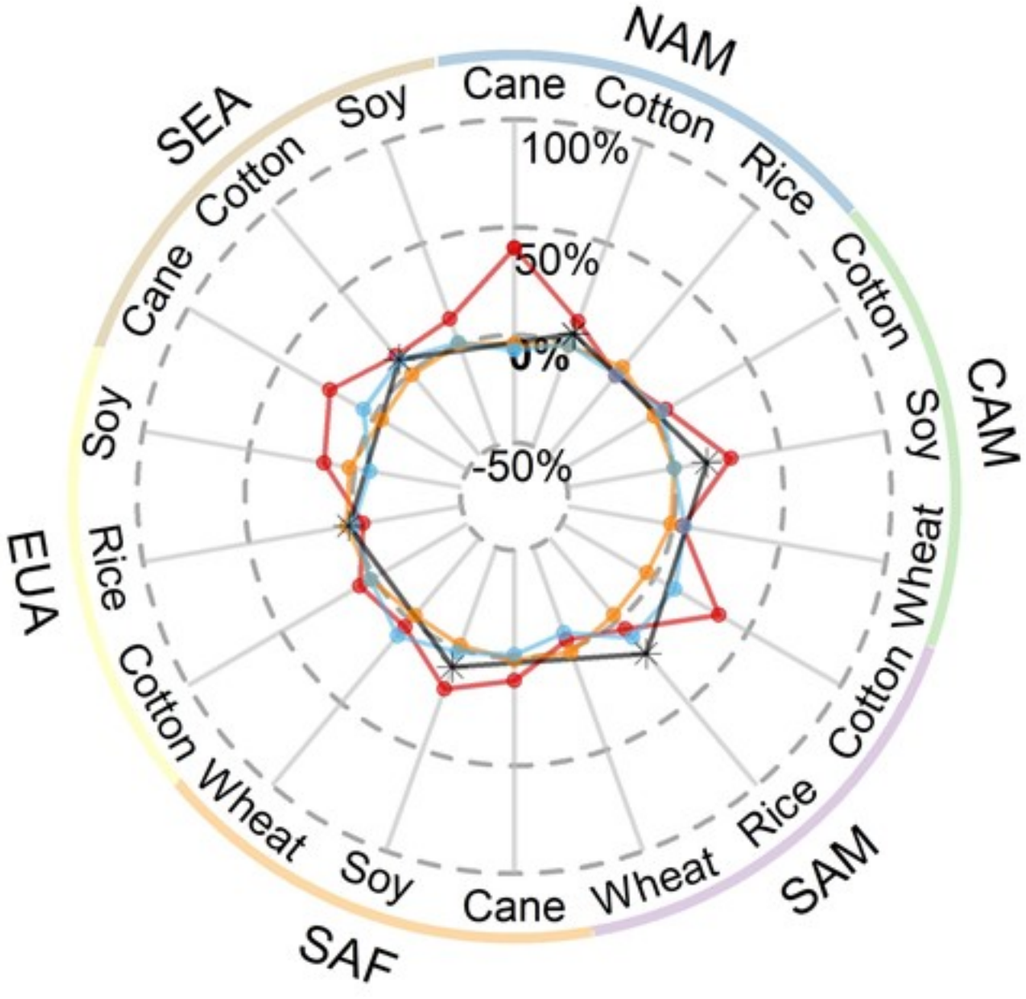


**c** CCT - RCP85

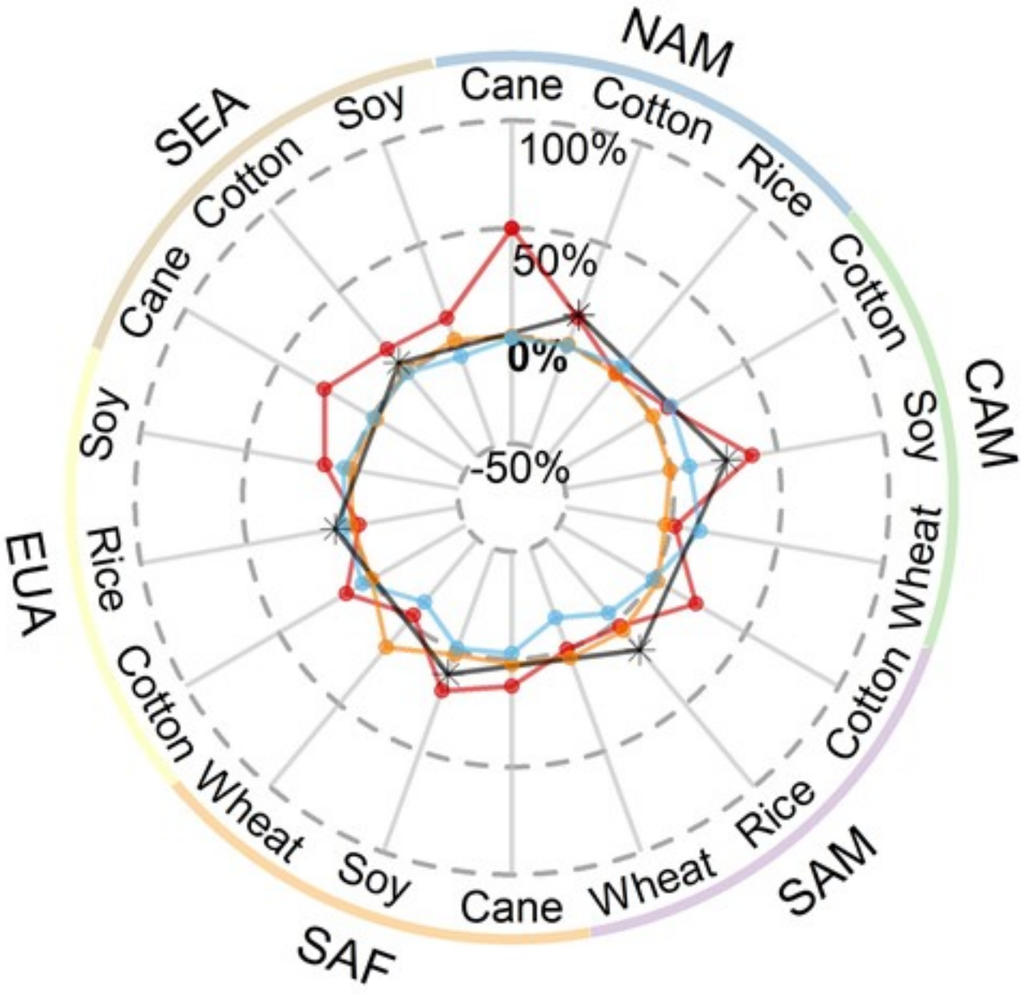


**d** Emissions reduction

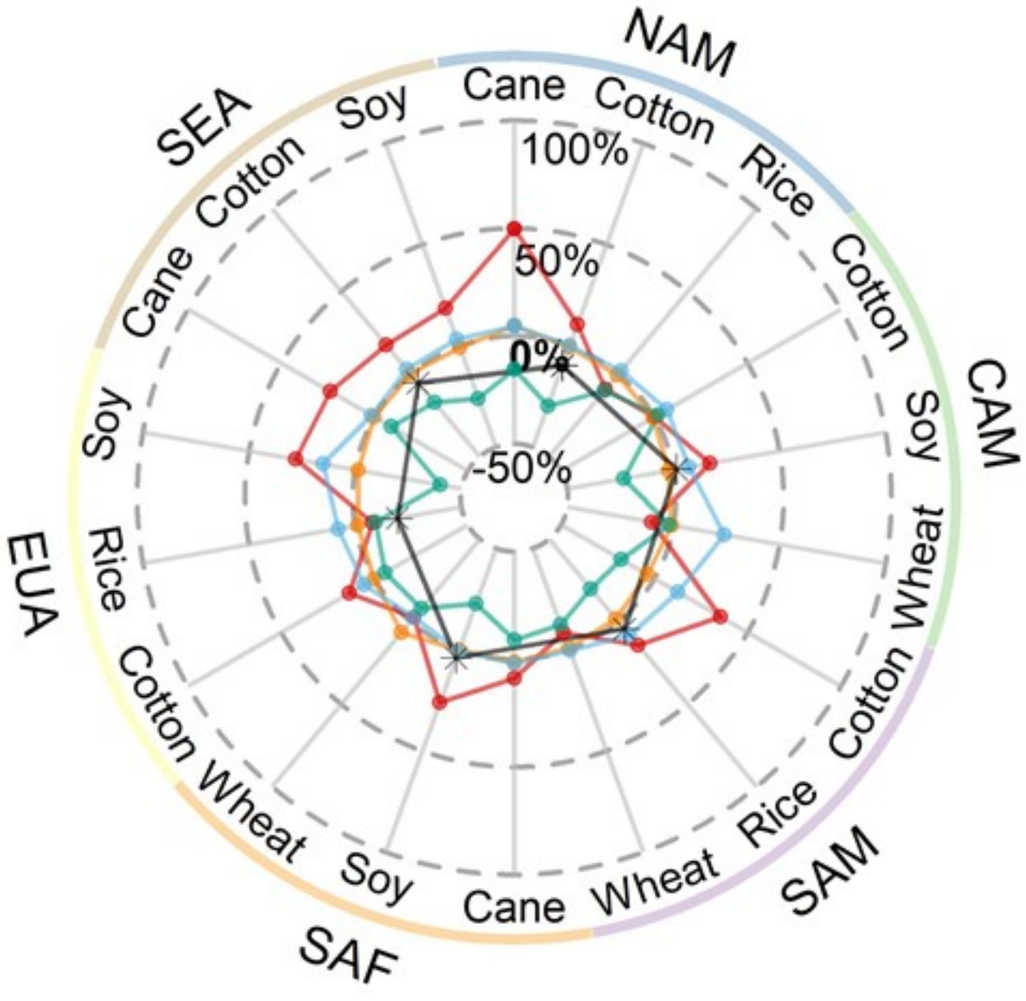


Temperature effect
Radiation effect
Moisture effect
$CO_2$ effect
Regional total effect

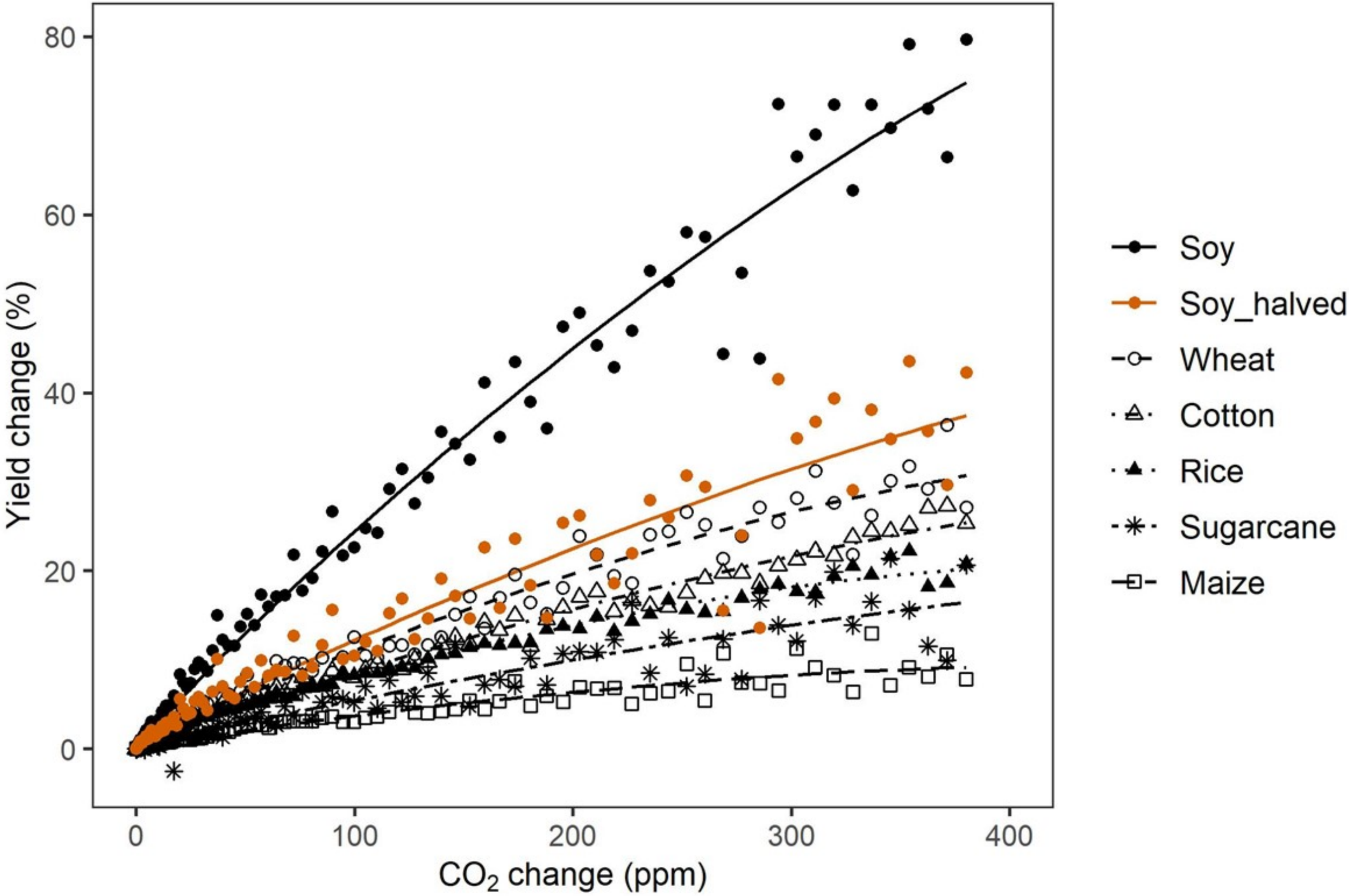
80
60
40
20
0
Yield change (%)
0
100
200
300
400
CO2 change (ppm)
Soy
Soy_halved
Wheat
Cotton
Rice
Sugarcane
Maize

**a**

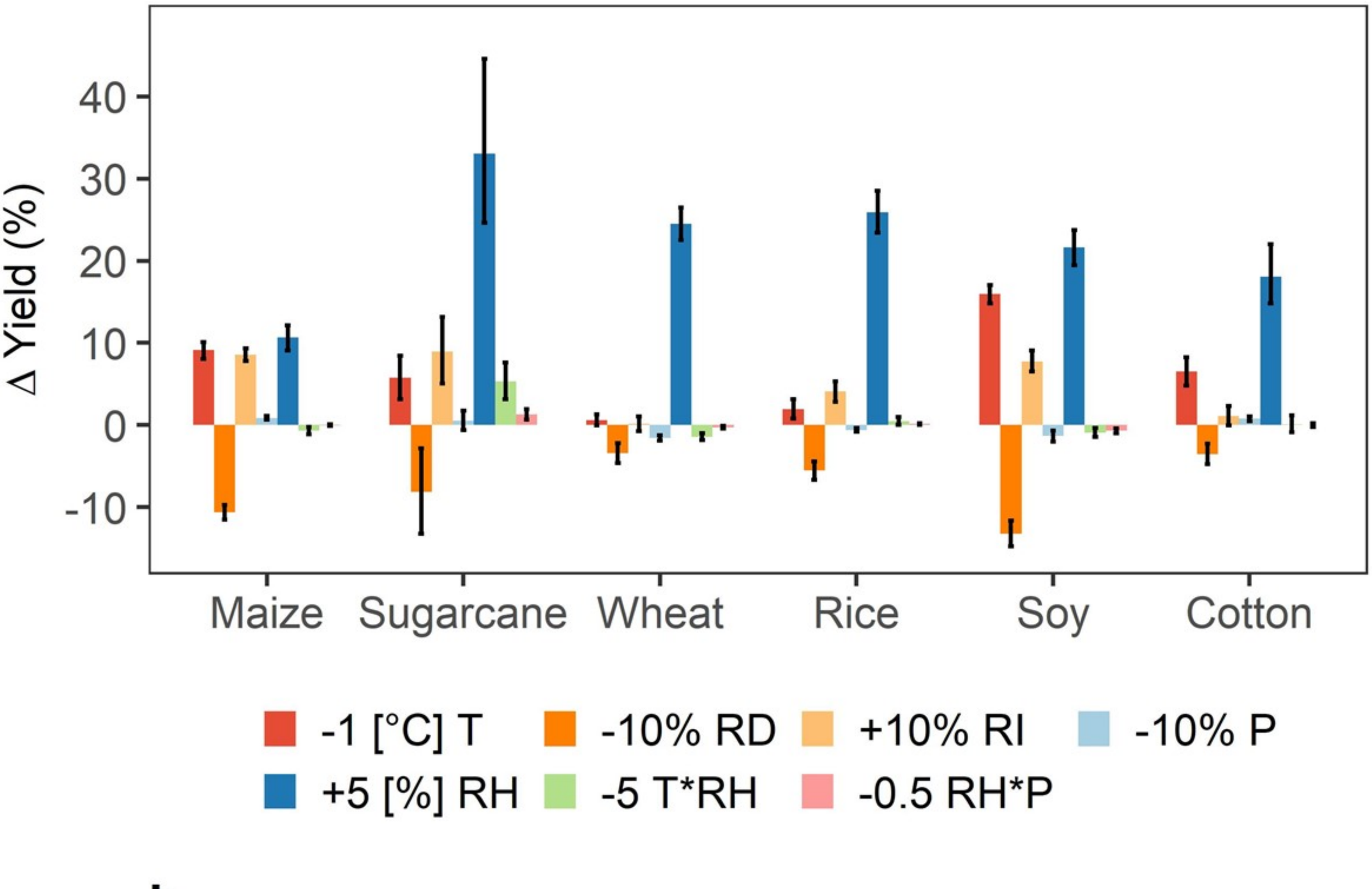
Δ Yield (%)
40
30
20
10
0
-10
Maize
Sugarcane
Wheat
Rice
Soy
Cotton
-1 [°C] T
-10% RD
+10% RI
-10% P
+5 [%] RH
-5 T*RH
-0.5 RH*P

**b**

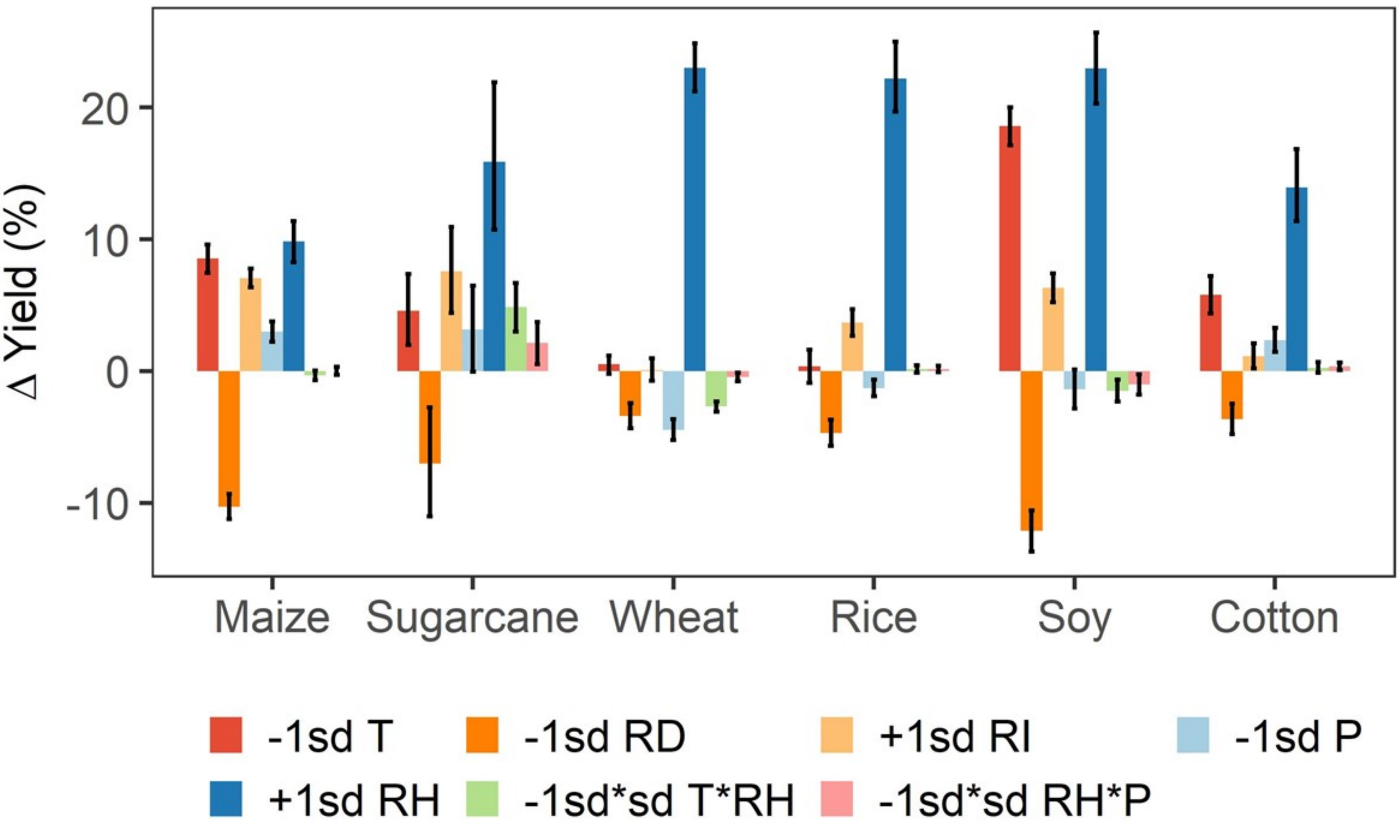
Δ Yield (%)
20
10
0
-10
Maize
Sugarcane
Wheat
Rice
Soy
Cotton
-1sd T
-1sd RD
+1sd RI
-1sd P
+1sd RH
-1sd*sd T*RH
-1sd*sd RH*P